Arbeit zur Erlangung des akademischen Grades Master of Science (M.Sc.)
im Studiengang Physik

Aspects of the Gauge Hierarchy of the Standard Model

eingereicht von Richard Schmieden

geb. am 07.03.1996 in Bad Kreuznach

FRIEDRICH-SCHILLER-
UNIVERSITÄT
JENA

Jena, November 23, 2020

Betreut durch: Dr. Luca Zambelli und Prof. Dr. Holger Gies

Erstgutachter: Prof. Dr. Holger Gies

Zweitgutachter: Dr. Luca Zambelli

Aspects of the Gauge Hierarchy of the Standard Model

Abstract

The standard model (SM) is a huge success, being able to explain particle physics phenomenology up to the energy scales accessible nowadays (up to 13 TeV). Albeit this huge feat, the SM is not considered to provide an ultimate description of nature. Many extensions of the standard model have been motivated by the so-called hierarchy problem. While this does not characterize an incosistency of the standard model, it rather refers to the aesthetics of the theory, or its naturalness. This issue is often paraphrased as: How can the Higgs mass m_{H}^2 stay small compared to the UV cutoff Λ while it receives radiative corrections which are naively of order $\sim \Lambda^2$? One way out of this predicament is to choose the initial conditions m_Λ^2 at a high-energy scale Λ really precisely so that these radiative corrections get cancelled. This procedure is known as fine-tuning.

In this work functional renormalization group techinques are employed to provide a new perspective on the gauge hierarchy of various toy models mimicking parts of the standard model. First a $\mathbb{Z}_2$-symmetric toy model containing one real scalar field and one Dirac fermion is studied, especially focussing on the dependence of the scale separation on the IR observables top mass and Higgs mass. Then a model containing $N_{\mathrm{f}} = 6$ Fermions transforming in the fundamental representation of SU(3), gauge bosons, and one scalar SU(2) doublet is investigated. The strong interaction forces spontaneous chiral symmetry breaking which will be accounted for by partial bosonization of the theory, in addition to the the usual electroweak symmetry breaking in the scalar sector. The hierarchy of the emerging scales is studied, namely the UV cutoff, the electroweak scale and in the latter model also the QCD scale for different values of the parameters of the models. The goal is to study the phase transition or crossover of this standard-model-like system from a "deeply-Higgsed" into a pure QCD-type phase. From the renormalization group perspective, the rapidness of this transition is quantitatively related to the severity of the naturalness problem.

Aspekte der Eichhierarchie des Standardmodells

Das Standardmodell (SM) ist ein großer Erfolg der Teilchenphysik, da es die Phänomenologie bis zu den heute zugänglichen Energieskalen (bis zu 13 TeV) erklären kann. Trotz dieser Leistung wird das SM nicht als entgültige Beschreibung der

Natur angesehen. Viele Erweiterungen des Standardmodells wurden durch das sogenannte Hierarchieproblem im Standardmodell motiviert. Dies charakterisiert zwar keine Inkonsistenz des Standardmodells, bezieht es sich doch eher auf seine Ästhetik oder Natürlichkeit. Dieses Problem lässt sich gut durch die Frage, warum die Masse des Higgs-Bosons klein im Vergleich zu einer Hochenergie-(UV)-skala Λ ist, obwohl es naiv Strahlungskorrekturen von Ordnung Λ^2 erhällt, zusammenfassen.
Ein Weg dieses Problem zu umgehen besteht darin, die Anfangsbedingugnen an dieser Hochenergieskala so zu wählen, dass diese Quantenkorrekturen keinen Einfluss auf die Higgsmasse haben. Dieses Vorgehen ist als Feinabstimmung bekannt. In dieser Arbeit werden Methoden der funktionalen Renormierungsgruppe benutzt, um neue Blickwinkel auf die Eichhierarchie in verschiedenen, an Teile des Standardmodells erinnernde, Spielzeugmodellen zu erhalten. Zuerst wird ein $\mathbb{Z}_2$ symmetrisches Yukawamodell mit einem reellen Skalarfeld und einem Dirac Fermion mit besonderem Augenmerk auf die Abhängigkeit der Separation der UV Skala von der Fermiskala von den Observablen Higgsmasse und Topmasse untersucht. Dann wird ein Modell mit Eichfeldern, $N_\mathrm{f} = 6$ Fermionen, die unter der fundamentalen Repräsentation der Eichgruppe SU(3) transformieren, und einem komplexen skalaren SU(2)-Doublett untersucht. Die starke Wechselwirkung führt, zusätzlich zu der bereits bekannten elektroschwachen Symmetriebrechung des Skalarfeldes, zu spontaner chiraler Symmetriebrechung, die mit Hilfe von bosonischen Hilfsfeldern untersucht wird. Die Hierarchie der auftretenden Skalen, einerseits die Hochenergieskala, andererseits die elektroschwache Skala und die Skala der chiralen Symmetriebrechung, werden für unterschiedliche Parameterregionen untersucht. Das Ziel ist, den Phasenübergang, beziehungsweise den crossover-Übergang, dieser standardmodellartigen Theorien, von einer “tief gehiggsten” zu einer reinen QCD-artigen Phase zu untersuchen. Aus renormierungsgruppentheoretischen Überlegungen ist die Geschwindigkeit dieses Übergangs quantitativ mit dem Natürlichkeitsproblem verknüpft.

Contents

1 Introduction

The standard model (SM) of particle physics is a huge success, being able to capture elementary particle phenomenology up to energy scales accessible to present day colliders (around 13 TeV). The last building block of the SM to be detected was the Higgs boson, being discovered in 2012 [1, 2].
The theoretical foundations for this discovery were laid by Brout, Englert and Higgs [3–6], introducing a mechanism to generate masses for gauge bosons as well as fermions through spontaneous symmetry breaking. This was then used by Weinberg and Salam [7, 8] to unify the electromagnetic and weak interaction. Together with a description for the strong interaction [9–12] found in the seventies, this completes the current version of the SM. Despite these achievements, the standard model is nowadays regarded as being an effective field theory, perfectly applicable for energies achievable in present day experiments, but not extendible to arbitrary high scales. Even within the SM there are unresolved problems, some of which are tied to the scalar nature of the Higgs field. One of these is the so-called naturalness problem which concerns the large separation of a UV scale (in the SM this is thought to be the Planck scale) and the Fermi scale, which sets the magnitude of masses in the IR. In order to achieve the large separation over several orders of magnitude, as is observed in the SM, a high degree of fine-tuning of the Higgs mass parameter is necessary. Since no symmetry protects the Higgs mass against radiative corrections, the Higgs mass parameter is naively expected to be of the order of the UV cutoff scale. The goal of this work is to shed some light on the fine-tuning problem, with special focus on how the strong gauge sector, based on the symmetry group $\mathrm{SU}(N_\mathrm{c})$, influences this necessity.
First we investigate a simple toy model, containing a scalar field and a Dirac fermion, playing the role of the Higgs boson and top quark, respectively. We employ functional renormalization group methods to gain insight on the dependence of the scale separation on different parameters in the theory, most notably the IR observables top and Higgs mass. We then turn towards a more complex

toy model, including gauge interactions mimicking the strong interaction in the standard model. We use effective field-theoretical methods, in particular partial bosonization, to connect high energy degrees of freedom of the strong interactions (quarks and gluons) with macroscopic degrees of freedom (fermionic bound states). The influence of this strong gauge sector on the fine-tuning problem is analyzed .

2 The Functional Renormalization Group Method

2.1. Functionals in QFT

In the following section we give a very basic introduction to quantum field theory through the method of functionals. We present some tools necessary to understand the following chapters. For a more thorough introduction to functionals in QFT we refer the reader to standard textbooks such as [13–15].
The basic object of this section is a general field ϕ which lives on a flat Euclidean spacetime. We therefore look at Euclidean field theories. We will assume that the results obtained in the Euclidean signature are transferable to a Minkowskian field theory via analytical continuation/Wick rotation.
The physical content of a field theory is stored in correlation functions of the field ϕ. In a (Euclidean) field theory, these n-point functions are obtained from the product of n field operators at different points A_n averaged over all possible field configurations. This weight is given by the exponential of the action $S[\phi]$, thus we get

$$G^{(n)}_{A_1,\cdots,A_n} = \langle \phi_{A_1} \cdots \phi_{A_n} \rangle \coloneqq \frac{1}{Z} \int \mathcal{D}\phi \, \phi_{A_1} \cdots \phi_{A_n} \mathrm{e}^{-S[\phi]}, \tag{2.1}$$

where Z is a normalization factor such that $\langle 1 \rangle = 1$. The labels A_i contain the spacetime coordinates as well as any internal indices of the i-th field

$$A_i = (x_i, a_i)\,. \tag{2.2}$$

Throughout this section we employ the Einstein summation convention if an index A appears twice. The inner product of two fields ϕ and ψ (which have the same type of indices) is then given by

$$\phi^A \psi_A = \int \mathrm{d}^d x \sum_a \phi^a(x) \psi_a(x). \tag{2.3}$$

The normalization factor in Eq (2.1)

$$Z = \int \mathcal{D}\phi \, \mathrm{e}^{-S[\phi]} \tag{2.4}$$

is sometimes called partition function of the theory, in analogy to statistical physics. We then modify the action by coupling a source term J^A linearly to the field

$$Z[J] = \int \mathcal{D}\phi \mathrm{e}^{-S[\phi]+J^A\phi_A} \tag{2.5}$$

which is now a functional depending on the source J. It is obvious that $Z[J]$ is the generator of the correlators. We get

$$\langle \phi_{A_1} \cdots \phi_{A_n} \rangle = \frac{1}{Z} \frac{\delta^n}{\delta J^{A_1} \cdots \delta J^{A_n}} Z\,[J]\Big|_{J\to 0} . \tag{2.6}$$

In most of the literature, this source-dependent functional $Z[J]$ is called partition function, and Z is just the normalization. One can furthermore get J-dependent expectation values simply by keeping the J dependence

$$\langle \phi_{A_1} \cdots \phi_{A_n} \rangle_J = \frac{1}{Z} \frac{\delta^n}{\delta J^{A_1} \cdots \delta J^{A_n}} Z[J] \, . \tag{2.7}$$

Another possibility to store the physical content of the theory is through a different functional, related to the partition by

$$W[J] = \log Z[J] \, . \tag{2.8}$$

$W[J]$ is often called generator of the connected n-point functions, although the nature of this name is quite elusive without having built a diagrammatic expansion. These connected n-point functions are again obtained by differentiation of a functional, this time of $W[J]$

$$G^{(n)}_{\text{conn.}} = \frac{\delta^n}{\delta J^{A_1} \cdots \delta J^{A_n}} W[J]\Big|_{J\to 0} . \tag{2.9}$$

We still have to introduce one more, and regarding the next section perhaps even more important, functional. For this we consider the J-dependent 1-point function of our theory

$$\varphi_A \coloneqq \langle \phi_A \rangle_J = \frac{\delta}{\delta J^A} W[J] \tag{2.10}$$

which defines the field φ_A. This field, called the classical field, can be seen as the thermodynamic variable conjugate to the source J^A. It is averaged over all possible

field fluctuations. Note that φ_A depends on the external source J^A. With this in mind, we can perform a Legendre transform of $W[J]$

$$\Gamma[\varphi] = \sup_J \left\{ \varphi_A J^A - W[J] \right\}, \tag{2.11}$$

where a special $J^A = J^A[\varphi]$ gets singled out such that Γ approaches its supremum. This transform is called effective action. From this definition of $\Gamma[\varphi]$ it immediately follows that Γ is convex.
As well as with the other functionals, Γ is also a generating functional and its correlators are given by

$$\Gamma^{(n)}_{A_1,\cdots,A_n} = \frac{\delta^n}{\delta\varphi_{A_1}\cdots\delta\varphi_{A_n}}\Gamma[\varphi]\,. \tag{2.12}$$

In a diagrammatic expansion one may see that these $\Gamma^{(n)}$ are the so called one particle irreducible (1PI) correlation functions. These are the proper vertices of the quantum theory. A proper vertex is a connected function, generated by $W[J]$, once all external lines have been removed. The meaning of the generating functional Γ becomes clear by studying its derivative

$$\frac{\delta\Gamma[\varphi]}{\delta\varphi_A} = -\frac{\delta W[J]}{\delta J^B}\frac{\delta J^B}{\delta\varphi_A} + \frac{\delta J^B}{\delta\varphi_A}\varphi_B + J^A = J^A, \tag{2.13}$$

which is the quantum equation of motion. Γ is the classical action capable of reproducing the quantum correlations.
From the definition of $Z[J]$ we can directly derive an expression for Γ

$$\mathrm{e}^{-\Gamma[\varphi]} = \int \mathcal{D}\phi \exp\left\{ -S[\varphi+\phi] + \int \frac{\delta\Gamma[\varphi]}{\delta\varphi_A}\phi_A \right\}. \tag{2.14}$$

Expanding this equation in powers of the field φ_A results in an infinite tower of coupled differential equations, the so called Dyson-Schwinger equations. The computation of the effective action is by no means a trivial task, and exact solutions for Γ have so far only been found in a few special cases.

2.2. Functional Renormalization

One feature of QFT is that the coupling constants are in fact not constant but they are scale dependent. Rather than an emergent scale dependence like in pertubation theory, we look at scale-dependent functionals so that this characteristic is built into the formalism from the beginning. The idea of the functional renormalization group is heavily rooted in the Wilsonian approach to renormalization which we will

sketch in the following [16].
For simplicity, we consider a scalar field on a d-dimensional Euclidean spacetime. We expand the field in the momentum basis

$$\phi(x) = \int \frac{\mathrm{d}^d q}{(2\pi)^d} \phi(q) \mathrm{e}^{-\mathrm{i}qx} \equiv \int_q \phi_q \mathrm{e}^{-\mathrm{i}qx} \tag{2.15}$$

and have a functional measure for our field integration in the partition function

$$\mathcal{D}\phi = \prod_{q \in \mathbb{R}^d} \mathrm{d}\phi_q. \tag{2.16}$$

The partition function obtained as in the previous section (c.f. Eq. (2.4)) can be ill defined because generally the field can have infinitely many modes. Such divergences arise from the unbounded integration in momentum space, a straightforward way to deal with this is to introduce a cutoff Λ and an action $S_\Lambda[\phi]$ such that

$$Z = \int \prod_{|q| \leq \Lambda} \mathrm{d}\phi_q \mathrm{e}^{-S_\Lambda[\phi]}. \tag{2.17}$$

The introduced cutoff regularizes the divergent correlations so that we can work with finite expressions. The regularized action S_Λ on the other hand is needed in order to obtain the same partition function as without the modifications. $S_\Lambda[\phi]$ is then viewed as a certain UV action containing the information of our theory at large energies, or therefore short distances due to the dual relation. This makes sense if we have a very large scale Λ above which the behavior of this theory is unknown. Since the introduced cutoff is arbitrary, nothing stops us from considering any scale k and writing the partition function according to Eq. (2.17) as

$$Z = \int \prod_{|q| \leq k} \mathrm{d}\phi_q \mathrm{e}^{-S_k[\phi]}. \tag{2.18}$$

This introduces a semigroup-like structure, and we are able to relate $S_k[\phi]$ to $S_\Lambda[\phi]$, since

$$Z = \int \prod_{|q| \leq k} \prod_{k \leq |q| \leq \Lambda} \mathrm{d}\phi_q \mathrm{e}^{-S_\Lambda[\phi]} \tag{2.19}$$

gives us the relation

$$\mathrm{e}^{-S_k[\phi]} = \int \prod_{k \leq |q| \leq \Lambda} \mathrm{d}\phi_q \mathrm{e}^{-S_\Lambda[\phi]}. \tag{2.20}$$

The interpretation of this is that $S_\Lambda[\phi]$ is the UV action and $S_k[\phi]$ is (with a slight abuse of nomenclature) an effective action, the so-called Wilsonian effective action, obtained by integrating out all modes with momentum $k \leq |q| \leq \Lambda$ towards the

IR. Once we have integrated out all momenta, we are left with a theory in which all scales contribute to the understanding of the theory. While in the Wilsonian approach this coarse graining results in a loss of information of microscopical degrees of freedom and thus gives us an effective theory for slow modes, in the functional renormalization group we start with an appropriate truncation at a high energy scale (the UV cutoff Λ) and freeze out the propagation of slow modes up to an infrared cutoff k. Letting this cutoff go to zero, we include these low-energy modes, thus including long range effects to the theory. The low-energy physics thus gets determined only by the microscopical degrees of freedom, arising dynamically by integrating out high-energy modes.
This problem is well posed if one considers the evolution from high to low energies, but problems may arise when evolving the system in the opposite direction. For $\Lambda \to \infty$, the existence of irrelevant couplings in the theory is such a case, since these generally become negligible when going from the UV to the IR, independent of their initial condition at the high energy scale. Conversely you can say that switching up the direction of the renormalization group in that case can then lead to huge numerical errors. Another case where we can't solve the flow from the IR (where we have taken the limit $k \to 0$) to the UV is when there is an IR attractive fixed-point structure such that the model "looses its memory", meaning regardless of the initial conditions chosen in the high energy regime the coupling will be attracted to the fixed-point value and a reversal of the flow is not well defined. If we never actually perform the limits $\Lambda \to \infty$ or $k \to 0$ we will not encounter these problems, and switching up the direction of the flow poses no problems.
We start, as in the previous example, by further modifying the partition function. We add an infrared cutoff depending on some scale k, which is often called sliding scale, and we return to the general notation of the previous section,

$$Z_k[J] = \int \mathcal{D}\phi \, \mathrm{e}^{-S[\phi] + J^A \phi_A - \Delta S_k[\phi]}. \tag{2.21}$$

The new term $\Delta S_k[\varphi]$ is quadratic in the fields and can therefore be viewed as a scale-dependent mass term for the fields, suppressing the propagation of φ_A modes with momentum smaller than k

$$\Delta S_k[\phi] = \frac{1}{2} \, \phi_A R_k^{AB} \phi_B. \tag{2.22}$$

The here introduced regulator function $R_k^{AB} = R_k^{ab}(p) \, \delta_{p,-q}$ should satisfy [17]

- $R_{k=0}^{ab}(p) = 0$. This ensures that the regulator vanishes for $k \to 0$, meaning we automatically recover the standard generating functional $\Gamma_{k=0} = \Gamma$.
- $R_{k \to \Lambda \to \infty}^{ab}(p) \to \infty$, implying that the functional integration is dominated by the stationary point of the action, justifying a saddle-point approximation yielding the classical action up to an additive constant $\Gamma_{k \to \Lambda} \to S$.

- $R_k^{ab}(p) \sim 0$ for $p > k$, thus leaving the fast modes unaffected by this modification.
- $R_k^{ab}(p) > 0$ for $p < k$, meaning R_k^{ab} acts as an IR regulator of the propagators.

These conditions ensure that we end up with an interpolating functional Γ_k, called effective average action, which for $k \to 0$ equals the full quantum action Γ and in the case of $k \to \Lambda$ approaches the classical action.
To derive a flow equation we start constructing the effective functionals like in the previous section. We introduce the notations

$$t = \log \frac{k}{\Lambda}, \qquad \partial_t = k \frac{\mathrm{d}}{\mathrm{d}k}, \tag{2.23}$$

where t is sometimes called renormalization group (RG) time, and start with the functional $W_k[J]$. For a k-independent source J we get

$$\begin{aligned} \partial_t W_k[J] &= \partial_t \log Z_k[J] \\ &= -\frac{1}{2} \int_p \int \mathcal{D}\phi \, \phi_a(-p) \, \partial_t R_k^{ab}(p) \, \phi_b(p) \, \mathrm{e}^{-S - \Delta S_k + J^A \phi_A} \\ &= -\frac{1}{2} \int_p \partial_t R_k^{ab}(p) \, \langle \phi_a(-p) \, \phi_b(p) \rangle . \end{aligned} \tag{2.24}$$

The 2-point function can be written in terms of functional derivatives of $W_k[J]$ and with the fact that J derivatives are only acting on the functionals, since the k derivative is taken at fixed J, we arrive at

$$\partial_t W_k[J] = -\frac{1}{2} \partial_k R_k^{AB} \left(\frac{\delta^2 W_k[J]}{\delta J^A \delta J^B} + \frac{\delta W_k[J]}{\delta J^A} \frac{\delta W_k[J]}{\delta J^B} \right). \tag{2.25}$$

This is a functional differential equation for the scale dependence of $W_k[J]$. From here we are able to obtain the evolution of $\Gamma_k[\varphi]$. As in the previous section we define the classical field φ_A as

$$\varphi_A = \langle \phi_A \rangle_J = \frac{\delta W_k[J]}{\delta J^A}. \tag{2.26}$$

Note that, since we are interested in studying $\Gamma_k[\varphi]$ as a functional of a k-independent field, the source is necessarily scale dependent. Γ_k is then defined via a slightly modified Legendre transform

$$\Gamma_k[\varphi] = \sup_J \left\{ \varphi_A J^A - W_k[J] \right\} - \Delta S_k[\varphi] . \tag{2.27}$$

This has straightforward consequences for the equations derived in the previous section. The quantum equation of motion has an additional regulator insertion

$$J^A = \frac{\delta \Gamma_k [\varphi]}{\delta \varphi_A} + R_k^{AB} \varphi_B. \tag{2.28}$$

From this it immediately follows that

$$\frac{\delta J^A}{\delta \varphi_B} = \frac{\delta^2 \Gamma_k [\varphi]}{\delta \varphi_A \delta \varphi_B} + R_k^{AB}. \tag{2.29}$$

But from Eq. (2.26) we also get

$$\frac{\delta \varphi_A}{\delta J^B} = \frac{\delta^2 W_k [J]}{\delta J^A \delta J^B}. \tag{2.30}$$

Combining these two results yields

$$\delta(A - C) = \frac{\delta J^A}{\delta J^C} = \frac{\delta J^A}{\delta \varphi_B} \frac{\delta \varphi_B}{\delta J^C} = \left(\Gamma_k^{(2)} + R_k\right)^{AB} \left(W_k^{(2)}\right)_{BC}, \tag{2.31}$$

where we have introduced the condensed notation

$$\left(\Gamma_k^{(n)}\right)^{A_1 \cdots A_n} = \frac{\delta^n \Gamma_k [\varphi]}{\delta \varphi_{A_1} \cdots \delta \varphi_{A_n}} \tag{2.32}$$

for the functional Γ_k and similarly for the generating functional $W_k [J]$. The delta function of the abstract indices is given by

$$\delta(A - B) = \delta_{ab} \delta(x - y). \tag{2.33}$$

With all these results, acting with ∂_t on Eq. (2.27) gives us the flow equation of Γ_k for fixed φ [18–21]:

$$\begin{aligned}
\partial_t \Gamma_k [\varphi] &= - \partial_t W_k [J]|_\varphi + (\partial_t J)^A \varphi_A - \partial_t \Delta S_k [\varphi] \\
&= - \partial_t W_k [J]|_J - \partial_t \Delta S_k [\varphi] \\
&= \frac{1}{2} \partial_t R_k^{AB} \left(W_k^{(2)}\right)_{BA} \\
&= \frac{1}{2} \partial_t R_k^{AB} \left(\Gamma_k^{(2)} + R_k\right)^{-1}_{BA} \\
&= \frac{1}{2} \mathrm{STr} \left[\partial_t R_k \left(\Gamma_k^{(2)} [\varphi] + R_k\right)^{-1}\right].
\end{aligned} \tag{2.34}$$

The third equality holds since $\Delta S_k [\varphi] = \frac{1}{2} R_k^{AB} \left(\frac{\delta W_k [J]}{\delta J^A} \frac{\delta W_k [J]}{\delta J^B}\right)$ cancels the appropriate term in Eq. (2.25), the next equality follows directly from Eq. (2.31). The

STr stands for Supertrace, denoting a trace over all internal as well as spacetime indices, additionally containing a negative sign for Grassmann-valued fields.
Equation (2.34) is known as the Wetterich equation which is an exact equation of the functional renormalization group. Since the term within the round parentheses is the kinetic term of the full regularized theory, its inverse represents the full propagator. The Wetterich equation therefore possesses a one-loop structure which eases computations. Nevertheless, this one-loop form does not come from an approximation since in the derivation no expansion of the path integral was performed. We are thus able to represent equation (2.34) diagramatically as shown in Figure 2.1. Note that this is a functional differential equation which does not

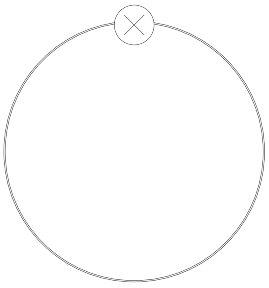

Figure 2.1.: Diagrammatic representation of the RHS of Eq. (2.34) (without prefactor of 1/2). The renormalization group flow of Γ_k is given as a one-loop form, here the line does not represent the free propagator like in usual Feynman diagrams, but denote the fully dressed propagator at scale k $G_k = (\Gamma_k^{(2)} + R_k)^{-1}$ of the theory. The insertion of $\partial_t R_k$ is diagrammatically represented by the crossed circle.

depend on any truncation of the effective average action. It thus contains all operators which are compatible with the symmetries of our theory. Since this number is usually infinite, we have to introduce a truncation of the effective average action Γ_k to do actual computations (meaning we restrict ourselves to a managable amount of operators, often sorted by their mass dimensions). The flow equations for the different operators then get extracted from the Wetterich equation by applying the appropriate projection rule for the operators on Eq. (2.34). There is however a scheme dependence involved, stemming from the regulator function which only has to obey the previously mentioned properties. This problem is resolved when looking at the end points of the trajectory ($k = 0$ or $k \to \Lambda$), since these points are universal. The Wilsonian idea to integrate momentum shell by momentum shell is also incorporated into this technique through the regulator. The insertion of R_k into the propagator screens slow modes in a mass-like fashion, while the derivative $\partial_t R_k$ suppresses modes with momenta larger than the reference scale k. The RG

flow can then be seen as a tool that connects theories valid at different scales in theory space.

3 Renormalization Group Equations for a Higgs-Yukawa Toy Model

3.1. Our Toy Model

In this section we introduce our Higgs-Yukawa toy model, intended to approximate the Higgs-top sector of the standard model and it will follow largely [22–24]. For now all other fermion flavors will be neglected, which is a reasonable first approximation since the top quark is so much heavier than the other quarks, implying a large top Yukawa coupling. Thus the main contribution to the beta functions stems from top fluctuations. The field content of our toy model therefore is one real scalar field as well as one Dirac fermion, representing the Higgs particle and the top quark, respectively. Our main points of interest are the scalar potential as well as the resulting particle masses in the IR, namely the Higgs and the top mass. We consider the minimal features necessary to reproduce the physical properties of our toy model. These are, namely, that bosonic and fermionic fluctuations drive the flow of the scalar effective potential through self interaction or Yukawa interaction, respectively, and the possibility to dynamically generate a vacuum expectation value (vev) in the scalar effective potential which implies a dynamical generation of a mass for the top quark. The shape of the potential then sets the Higgs mass while the vev as well as the IR value of the Yukawa coupling fix the fermion mass. In order to achieve this, we first need to make the fields dynamical, most easily done by introducing the classical kinetic terms for the bosonic field as $\frac{1}{2}\left(\partial_\mu \phi(x)\right)^2$ and the fermionic field by $\bar{\psi}(x)\mathrm{i}\partial\!\!\!/\psi(x)$. A generic mass term $\frac{1}{2}m^2\phi(x)^2$ for the scalar field is allowed while the fermion is protected against a mass term by chiral symmetry, solely acquiring its mass through the Yukawa interaction. Then the last operators needed to arrive at a suitable model are the scalar self-interaction, the simplest case being $\lambda\phi(x)^{2n}$ with $n > 1$, and a Yukawa interaction $\mathrm{i}\bar{h}\phi(x)\bar{\psi}(x)\psi(x)$. We allow only even powers of the scalar field due to the discrete chiral symmetry

of this model. With all this, we arrive at the Lagrangian of our toy model

$$\mathcal{L} = \frac{1}{2}\left(\partial_\mu \phi\right)^2 - U\left(\phi^2\right) + \bar{\psi}\mathrm{i}\partial_\mu \gamma^\mu \psi + \mathrm{i}\bar{h}\phi\bar{\psi}\psi. \tag{3.1}$$

Here $U(\phi^2)$ is the scalar potential. This model is $\mathbb{Z}_2$-invariant, meaning it is invariant under the discrete chiral symmetry

$$\psi \to \mathrm{e}^{\mathrm{i}\frac{\pi}{2}\gamma_5}, \qquad \bar{\psi} \to \bar{\psi}\mathrm{e}^{\mathrm{i}\frac{\pi}{2}\gamma_5}, \qquad \phi \to -\phi. \tag{3.2}$$

Since this symmetry is discrete, we do not gain any new massless Goldstone bosons by the spontaneous symmetry breaking from a nonzero vev of the scalar field $\langle\phi\rangle \neq 0$. This is also a property of the standard model, since there the massless modes are eaten by the massive electroweak gauge bosons.
With these considerations we arrive at the effective average action

$$\Gamma_k = \int_x \left[\frac{Z_{\varphi,k}}{2}\left(\partial_\mu \varphi(x)\right)^2 + U_k(\varphi(x)^2) + Z_{\psi,k}\bar{\psi}(x)\mathrm{i}\not{\partial}\psi(x) + \mathrm{i}\bar{h}_k\varphi(x)\bar{\psi}(x)\psi(x)\right], \tag{3.3}$$

where $\varphi(x)$ describes the excitation above the vacuum. In the case where the minimum of the potential is not at vanishing field we should split the scalar field as $\varphi(x) = \varphi_{\mathrm{vev}} + \Delta\varphi(x)$ where φ_{vev} is the vacuum expectation value of the scalar field. Since deriving the flow equations in momentum space is more convenient, we Fourier transform our effective action. With the conventions

$$\begin{aligned}
\varphi(x) &= \int_p \varphi(p)\mathrm{e}^{\mathrm{i}px}, \\
\psi(x) &= \int_p \psi(p)\mathrm{e}^{\mathrm{i}px}, \\
\bar{\psi}(x) &= \int_p \bar{\psi}(p)\mathrm{e}^{-\mathrm{i}px}
\end{aligned} \tag{3.4}$$

for the Fourier transform we get

$$\Gamma_k = \int_x U_k\left(\varphi(x)^2\right) + \int_p \left[\frac{Z_{\varphi,k}}{2}\varphi(p)p^2\varphi(-p) - Z_{\psi,k}\bar{\psi}(p)\not{p}\psi(p) + \int_q \mathrm{i}\bar{h}_k\varphi(q-p)\bar{\psi}(q)\psi(p)\right]. \tag{3.5}$$

3.2. Flow Equations of the Toy Model

For the derivation of the flow equations we first need the fluctuation matrix $\Gamma_k^{(2)}(p,q)$ for our toy model

$$\Gamma_k^{(2)}(p,q) = \begin{pmatrix} \frac{\overrightarrow{\delta}}{\delta\varphi(-p)} \\ \frac{\overrightarrow{\delta}}{\delta\psi^{\mathrm{T}}(-p)} \\ \frac{\overrightarrow{\delta}}{\delta\bar{\psi}(p)} \end{pmatrix} \Gamma_k \left(\frac{\overleftarrow{\delta}}{\delta\varphi(q)}, \quad \frac{\overleftarrow{\delta}}{\delta\psi(q)}, \quad \frac{\overleftarrow{\delta}}{\delta\bar{\psi}^{\mathrm{T}}(-q)}. \right).$$

Using the effective average action of our toy model (Eq. (3.5)) we get

$$\Gamma_k^{(2)}(p,q) = \begin{pmatrix} Z_{\varphi,k}p^2\delta_{p,q} \\ +\int_x U''(\varphi(x))\mathrm{e}^{\mathrm{i}(q-p)x} & \mathrm{i}\bar{h}_k\bar{\psi}(q-p) & -\mathrm{i}\bar{h}_k\psi^{\mathrm{T}}(p-q) \\ -\mathrm{i}\bar{h}_k\bar{\psi}^{\mathrm{T}}(q-p) & 0 & \begin{matrix} -Z_{\psi,k}\not{p}^{\mathrm{T}}\delta_{p,q} \\ -\mathrm{i}\bar{h}_k\varphi(p-q) \end{matrix} \\ \mathrm{i}\bar{h}_k\psi(p-q) & \begin{matrix} -Z_{\psi,k}\not{p}\delta_{p,q} \\ +\mathrm{i}\bar{h}_k\varphi(p-q) \end{matrix} & 0 \end{pmatrix}, \tag{3.6}$$

where primes denote derivatives with respect to φ. The last missing piece in order to evaluate Eq. (2.34) is the regulator matrix $R_k(p,q)$. Since we can implement this IR cutoff through regularizing the small-momentum regime, the regulator matrix should have nonzero entries for elements containing momentum dependences. The corresponding operators are φ^2 and $\bar{\psi}\psi$ (or $\psi^{\mathrm{T}}\bar{\psi}^{\mathrm{T}}$) for the scalar field and the fermionic field, respectively. Thus the regulator is given by

$$R_k(p,q) = \begin{pmatrix} R_{k,\mathrm{B}}(p) & 0 & 0 \\ 0 & 0 & -R_{k,\mathrm{F}}^{\mathrm{T}}(-p) \\ 0 & R_{k,\mathrm{F}}(p) & 0 \end{pmatrix} \delta_{p,q}. \tag{3.7}$$

Since the final flow equations are expressed in dimensionless, renormalized quantities, we write the regulator as

$$R_k(p,q) = \begin{pmatrix} Z_{\varphi,k} p^2 r_{k,\mathrm{B}}(p) & 0 & 0 \\ 0 & 0 & -Z_{\psi,k} \not{p}^{\mathrm{T}} r_{k,\mathrm{F}}(-p) \\ 0 & -Z_{\psi,k} \not{p} r_{k,\mathrm{F}}(p) & 0 \end{pmatrix} \delta_{p,q}, \tag{3.8}$$

where $r_{k,\mathrm{B}}$ and $r_{k,\mathrm{F}}$ are dimensionless bosonic and fermionic regulator shape functions. These functions only depend on the square of the momenta, $r_k(p) = r(p^2/k^2)$. The exact form of these regulator shape functions will not be given here, since we do not need them for the derivation of the flow. We can in the end make a particular choice of the regulator to evaluate the resulting integrals.

Scalar Potential

To get the flow equation of the scalar potential, we have to project onto the potential in the effective action. It is easy to see from Eq. (3.5) that we have to set $\varphi(x) = \varphi_0$ constant while the fermion field vanishes $\bar{\psi}(x) = \psi(x) = 0$. Thus we arrive at the flow equation of the scalar potential

$$\partial_t U_k = \frac{1}{2} \mathrm{STr} \left[\left(\partial_t R_k(p,q) \right) \left(\Gamma_k^{(2)}(q,p) + R_k(q,p) \right) \right] \Big|_{\substack{\varphi=\varphi_0 \\ \bar{\psi}=\psi=0}} . \tag{3.9}$$

First projecting onto the potential yields a fluctuation matrix which is diagonal in momentum space. Together with the regulator, this can then be directly inverted, and we get

$$\left(\Gamma_K^{(2)}(p,q) + R_k(p,q) \right)^{-1} = \begin{pmatrix} \frac{1}{Z_{\varphi,k} P(p) + U''(\varphi_0)} & 0 & 0 \\ 0 & 0 & -\dfrac{Z_{\psi,k} \left(1 + r_{k,\mathrm{F}}(p)\right)}{Z_{\psi,k}^2 P_{\mathrm{F}}(p) + \bar{h}_k^2 \varphi_0^2} \not{p} \\ & & -\dfrac{\mathrm{i} \bar{h}_k \varphi_0}{Z_{\psi,k}^2 P_{\mathrm{F}}(p) + \bar{h}_k^2 \varphi_0^2} \\ 0 & -\dfrac{Z_{\psi,k} \left(1 + r_{k,\mathrm{F}}(p)\right)}{Z_{\psi,k}^2 P_{\mathrm{F}}(p) + \bar{h}_k^2 \varphi_0^2} \not{p}^{\mathrm{T}} & 0 \\ & + \dfrac{\mathrm{i} \bar{h}_k \varphi_0}{Z_{\psi,k}^2 P_{\mathrm{F}}(p) + \bar{h}_k^2 \varphi_0^2} & \end{pmatrix} \delta_{p,q}$$

Here we have introduced the inverse average propagators $P(p) = p^2(1 + r_{k,\mathrm{B}}(p))$ and $P_{\mathrm{F}}(p) = p^2(1 + r_{k,\mathrm{F}}(p))^2$. We then multiply Eq. (3.10) with $(\partial_t R_k(q,p))$ which results in a diagonal operator. Performing the trace over the internal space, and realizing that the "Supertrace" gives a minus sign in the fermionic sector, gives us

$$\partial_t U_k = \frac{1}{2} Z_{\varphi,k} \int_p \frac{\partial_t R_{k,\mathrm{B}}(p)}{P(p) + Z_{\varphi,k}^{-1} U_k''} - d_\gamma Z_{\psi,k} \int_p \frac{(1 + r_{k,\mathrm{F}}(p))\, p^2 \partial_t \left(Z_{\psi,k} r_{k,\mathrm{F}}(p)\right)}{P_{\mathrm{F}}(p) + Z_{\psi,k}^{-2} \bar{h}_k^2 \varphi_0^2}, \tag{3.10}$$

where $d_\gamma = 2^{\lfloor d/2 \rfloor}$ denotes the dimension of the gamma matrices. Introducing dimensionless threshold functions $l_0^{(\mathrm{B})d}(\omega;\eta_\varphi)$ and $l_0^{(\mathrm{F})d}(\omega;\eta_\psi)$ for the momentum integration (see Appendix A) yields a more compact way of writing the flow equation,

$$\partial_t U_k = 2 v_d k^d \left[l_0^{(\mathrm{B})d} \left(k^{-2} Z_{\varphi,k}^{-1} \left(2\rho U_k'' + U_k'\right); \eta_\varphi \right) - d_\gamma l_0^{(\mathrm{F})d} \left(2k^{-2} Z_{\psi,k}^{-2} \rho \bar{h}_k^2; \eta_\psi \right) \right]. \tag{3.11}$$

Here we have introduced the anomalous dimensions of the respecive fields, defined by

$$\eta_{\varphi,k} = -\partial_t \log Z_{\varphi,k}, \qquad \eta_{\psi,k} = -\partial_t \log Z_{\psi,k}. \tag{3.12}$$

Here primes denote derivatives with respect to the invariant $\rho = \frac{1}{2}\varphi^2$ and $v_d^{-1} = 2^{d+1}\pi^{d/2}\Gamma\left[d/2\right]$. Implementing this, we need to rewrite this equation in a dimensionless form to represent the quantities by numbers. In order to do this, we divide all dimensionfull quantities by an appropriate power of our sliding scale k.

Dimensionless Form Through Running Scale Division

For this we define the renormalized, dimensionless field invariant by

$$\tilde{\rho} = Z_{\varphi,k} k^{2-d} \rho, \tag{3.13}$$

the renormalized, dimensionless Yukawa coupling by

$$h_k^2 = Z_{\varphi,k}^{-1} Z_{\psi,k}^{-2} k^{4-d} \bar{h}_k^2 \tag{3.14}$$

and finally the dimensionless potential as

$$u_k = k^{-d} U_k. \tag{3.15}$$

Using these relations we arrive at

$$\partial_t u_k = -d u_k + (d - 2 + \eta_\varphi)\, \tilde{\rho} u_k' + 2 v_d \left[l_0^{(\mathrm{B})d} \left(\left(2\tilde{\rho} u_k'' + u_k'\right); \eta_\varphi \right) - d_\gamma l_0^{(\mathrm{F})d} \left(2\tilde{\rho} h_k^2; \eta_\psi \right) \right]. \tag{3.16}$$

Here, primes denote derivatives with respect to the dimensionless invariant $\tilde{\rho}$. The first two terms arise from the differentiation of k^{-d} as well as the derivative acting on the field invariant via chain rule. This result agrees with [24] in the literature.

Yukawa Coupling

Now we derive the flow of the Yukawa coupling h_k^2. We look into the flow of the squared coupling owing to the $\mathbb{Z}_2$ symmetry of our model. Furthermore, to cover the case where the vacuum expectation value of the scalar field is nonzero, we split the scalar field into a background and a fluctuating field $\varphi = \varphi_{\text{vev}} + \Delta\varphi$. The fluctuating part $\Delta\varphi$ is interacting with the fermions while the vacuum expectation value results in a mass term for the fermions. The Yukawa coupling can thus be isolated by projecting onto $\Delta\varphi\bar{\psi}\psi$, resulting in a projection rule that reads

$$\bar{h}_k = \frac{1}{\mathrm{i}} \frac{\delta}{\delta\Delta\varphi(p')} \frac{\overrightarrow{\delta}}{\delta\bar{\psi}(p)} \Gamma_k \frac{\overleftarrow{\delta}}{\delta\psi(q)} \bigg|_{\substack{\Delta\varphi=\bar{\psi}=\psi=0 \\ p'=p=q=0}} . \tag{3.17}$$

For the flow, we use the corresponding flow equation

$$\partial_t \bar{h}_k = \frac{1}{2\mathrm{i}} \frac{\delta}{\delta\Delta\varphi(p')} \frac{\overrightarrow{\delta}}{\delta\bar{\psi}(p)} \mathrm{STr} \left[(\partial_t R_k) \left(\Gamma_k^{(2)} + R_k \right)^{-1} \right] \frac{\overleftarrow{\delta}}{\delta\psi(q)} \bigg|_{\substack{\Delta\varphi=\bar{\psi}=\psi=0 \\ p'=p=q=0}} . \tag{3.18}$$

This time we are not allowed to project before taking the functional derivative. The resulting fluctuation matrix is not diagonal in momentum space, so we can not directly invert it. However, from the projection rules we can see that only terms containing each field $\Delta\varphi$,$\bar{\psi}$ and ψ exactly once survive. We therefore rewrite the flow equation as

$$\partial_t \bar{h}_k = \frac{1}{2\mathrm{i}} \frac{\delta}{\delta\Delta\varphi(p')} \frac{\overrightarrow{\delta}}{\delta\bar{\psi}(p)} \mathrm{STr} \left[\tilde{\partial}_t \log \left(\Gamma_k^{(2)} + R_k \right) \right] \frac{\overleftarrow{\delta}}{\delta\psi(q)} \bigg|_{\substack{\Delta\varphi=\bar{\psi}=\psi=0 \\ p'=p=q=0}} , \tag{3.19}$$

where we have defined $\tilde{\partial}_t$ to act only on the t dependence of the regulator R_k. We then expand $\log\left(\Gamma_k^{(2)} + R_k\right)$ in powers of the fields while keeping the projection rules in mind. For this, the operator $\left(\Gamma_k^{(2)} + R_k\right)$ gets split up into a propagator and a field part:

$$\left(\Gamma_k^{(2)} + R_k\right) = \left(\Gamma_{k,0}^{(2)} + R_k\right) + \Delta\Gamma_k^{(2)}. \tag{3.20}$$

Here, $\left(\Gamma_{k,0}^{(2)} + R_k\right)$ contains the components independent of the fields while $\Delta\Gamma_k^{(2)}$ includes all the dependencies on the fields $\Delta\varphi$,$\bar{\psi}$ and ψ. Already keeping the split

of the scalar field $\varphi(p) = \varphi_{\mathrm{vev},k} + \Delta\varphi(p)$ in mind, we get

$$\left(\Gamma^{(2)}_{k,0} + R_k\right) =$$

$$= \begin{pmatrix} Z_{\varphi,k}p^2\left(1 + r_{k,\mathrm{B}}(p)\right) & 0 & 0 \\ \quad + U_k''(\varphi_{\mathrm{vev},k}) & & \\ 0 & 0 & -Z_{\psi,k}\not{p}^{\mathrm{T}}\left(1 + r_{k,\mathrm{F}}(-p)\right) \\ & & \quad - i\bar{h}_k\varphi_{\mathrm{vev,k}} \\ 0 & -Z_{\psi,k}\not{p}\left(1 + r_{k,\mathrm{F}}(p)\right) & 0 \\ & \quad + i\bar{h}_k\varphi_{\mathrm{vev},k} & \end{pmatrix}, \tag{3.21}$$

and

$$\Delta\Gamma^{(2)}_k = \begin{pmatrix} U_k'''(\varphi_{\mathrm{vev},k})\Delta\varphi(p-q) & \mathrm{i}\bar{h}_k\bar{\psi}(q-p) & -\mathrm{i}\bar{h}_k\psi^{\mathrm{T}}(p-q) \\ -\mathrm{i}\bar{h}_k\bar{\psi}^{\mathrm{T}}(q-p) & 0 & -\mathrm{i}\bar{h}_k\Delta\varphi(p-q) \\ \mathrm{i}\bar{h}_k\psi(p-q) & \mathrm{i}\bar{h}_k\Delta\varphi(p-q) & 0 \end{pmatrix}, \tag{3.22}$$

where we have neglected all terms except the first order in

$$\begin{aligned} &\int_x U_k''\left(\varphi_{\mathrm{vev},k} + \Delta\varphi(x)\right)\mathrm{e}^{\mathrm{i}(q-p)x} \\ &\quad = \int_x \left[U_k''(\varphi_{\mathrm{vev},k}) + U_k'''(\varphi_{\mathrm{vev},k})\Delta\varphi(x) + \dots\right]\mathrm{e}^{\mathrm{i}(q-p)x} \\ &\quad = U_k''(\varphi_{\mathrm{vev},k})\delta_{p,q} + U_k'''(\varphi_{\mathrm{vev},k})\Delta\varphi(p-q) + \dots, \end{aligned} \tag{3.23}$$

since higher powers of $\Delta\varphi$ do not survive the projection. The propagator in Eq. (3.21) is diagonal in momentum space and can thus be inverted. We already have inverted this matrix in the derivation of the flow equation of the scalar potential, where we simply have to replace $\varphi_0 \to \varphi_{\mathrm{vev},k}$.

We then rewrite the operator $\log\left(\Gamma_k^{(2)}+R_k\right)$ to make it expandable through

$$\begin{aligned}
&\mathrm{STr}\left[\tilde{\partial}_t \log\left(\Gamma_k^{(2)}+R_k\right)\right] = \mathrm{STr}\left[\tilde{\partial}_t \log\left(\Gamma_{k,0}^{(2)}+\Delta\Gamma_k^{(2)}+R_k\right)\right] \\
&= \mathrm{STr}\left[\tilde{\partial}_t \log\left\{\left(\Gamma_{k,0}^{(2)}+R_k\right)\left(1+\left(\Gamma_k^{(2)}+R_k\right)^{-1}\Delta\Gamma_k^{(2)}\right)\right\}\right] \\
&= \mathrm{STr}\left[\tilde{\partial}_t \log\left(\Gamma_{k,0}^{(2)}+R_k\right)\right] + \mathrm{STr}\left[\tilde{\partial}_t \log\left\{\left(1+\left(\Gamma_k^{(2)}+R_k\right)^{-1}\Delta\Gamma_k^{(2)}\right)\right\}\right]. \quad (3.24)
\end{aligned}$$

We Taylor expand the logarithm $\log(1+x) = x - \frac{1}{2}x^2 + \frac{1}{3}x^3 + \dots$. Realizing that only terms cubic in $\Delta\Gamma_k^{(2)}$ survive the projection, since it contains all fields exactly once, we can write the flow equation of the Yukawa coupling as

$$\partial_t \bar{h}_k = \frac{1}{6\mathrm{i}}\frac{\delta}{\delta\Delta\varphi(p')}\frac{\overrightarrow{\delta}}{\delta\bar{\psi}(p)}\mathrm{STr}\left[\tilde{\partial}_t\left\{\left(\Gamma_{k,0}^{(2)}+R_k\right)^{-1}\Delta\Gamma_k^{(2)}\right\}^3\right]\frac{\overleftarrow{\delta}}{\delta\psi(q)}\bigg|_{\substack{\Delta\varphi=\bar{\psi}=\psi=0\\ p'=p=q=0}}. \quad (3.25)$$

Calculating the cube of $\left(\Gamma_{k,0}^{(2)}+R_k\right)^{-1}\Delta\Gamma^{(2)}$ is straightforward, although tedious, and after performing the projection rules as well as the trace over the internal spaces we arrive at

$$\begin{aligned}
\partial_t \bar{h}_k = -\mathrm{i}\int_p \tilde{\partial}_t \Bigg\{ & \\
(a) \qquad & \left(\mathrm{i}\bar{h}_k\right)^3 \frac{1}{Z_{\varphi,k}P(p)+U_k''(\varphi_{\mathrm{vev},k})}\frac{1}{Z_{\psi,k}^2 P_{\mathrm{F}}(p)+\bar{h}_k^2\varphi_{\mathrm{vev},k}^2} \\
(b) \qquad & -\left(\mathrm{i}\bar{h}_k\right)^3 \frac{\varphi_{\mathrm{vev},k}U_k'''(\varphi_{\mathrm{vev},k})}{\left[Z_{\varphi,k}P(p)+U_k''(\varphi_{\mathrm{vev},k})\right]^2}\frac{1}{Z_{\psi,k}P_{\mathrm{F}}(p)+\bar{h}_k^2\varphi_{\mathrm{vev},k}^2} \\
(c) \qquad & +\left(\mathrm{i}\bar{h}_k\right)^5 \frac{2\varphi_{\mathrm{vev},k}^2}{Z_{\varphi,k}P(p)+U_k''(\varphi_{\mathrm{vev},k})}\frac{1}{\left[Z_{\psi,k}^2 P_{\mathrm{F}}(p)+\bar{h}_k^2\varphi_{\mathrm{vev},k}^2\right]^2}\Bigg\}.
\end{aligned} \quad (3.26)$$

The three different contributions to the RG flow can be represented diagrammatically. These diagrams are depicted in Figure 3.1. Owing to the $\mathbb{Z}_2$ symmetry of our system, the Yukawa coupling only appears in squares. Therefore, we consider the flow of $\bar{h}_k^2$ instead of $\bar{h}_k$ to make this dependence explicit. Using $\partial_t\bar{h}_k^2 = 2\bar{h}_k\partial_t\bar{h}_k$ as well as renormalized, dimensionless quantities $h_k^2 = Z_{\varphi,k}^{-1}Z_{\psi,k}^{-2}k^{d-4}\bar{h}_k^2$, $u_k = k^{-d}U_k$ and $\kappa_k = \frac{1}{2}Z_{\varphi,k}k^{2-d}\varphi_{\mathrm{vev},k}^2$ we arrive at

$$\begin{aligned}
\partial_t h_k^2 = &\left(d-4+\eta_\phi+2\eta_\psi\right)h_k^2 + 8h_k^4 v_d l_{1,1}^{(\mathrm{FB})d}\left(\omega_1,\omega 2,\eta_\psi,\eta_\phi\right) \\
&-\left[48\kappa_k u_k''\left(\kappa_k\right)+32\kappa_k^2 u_k'''\left(\kappa_k\right)\right]h_k^4 v_d l_{1,2}^{(\mathrm{FB})d}\left(\omega_1,\omega 2,\eta_\psi,\eta_\phi\right) \\
&-32h_k^6\kappa_k v_d l_{2,1}^{(\mathrm{FB})d}\left(\omega_1,\omega 2,\eta_\psi,\eta_\phi\right).
\end{aligned} \quad (3.27)$$

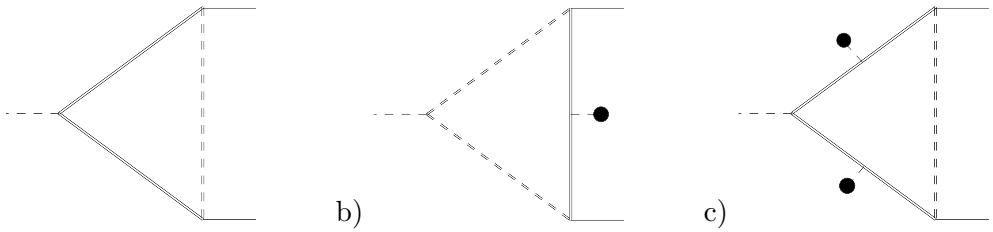

Figure 3.1.: Diagrammatic representation of the contributions to the flow equation of the Yukawa coupling (c.f. Eq. (3.26)). Coupling to the condensate $\varphi_{\mathrm{vev},k}$ is indicated by the black circle, regulator insertions are suppressed.

This agrees with the result found in [24].
Here we have again introduced a compact notation with threshold functions for the momentum integrations, and their definitions can be found in Appendix A. In Eq. (3.27) primes denote derivatives with respect to $\tilde{\rho} = \frac{1}{2} Z_{\varphi,k} k^{2-d} \varphi^2$, and the anomalous dimensions are, as before, defined by $\eta_{\varphi,k} = -\partial_t \log Z_{\varphi,k}$ and $\eta_{\psi,k} = -\partial_t \log Z_{\psi,k}$.

Anomalous Dimensions

The last ingredient needed for our set of equations are the flow equations of the field strength renormalizations $Z_{\varphi,k}$ and $Z_{\psi,k}$. It is possible to remove all explicit dependencies on these field renormalizations by introducing dimensionless, renormalized quantities and the anomalous dimensions, as we did for the previous cases. The final equations for the anomalous dimensions will be purely algebraic, meaning we don't have to state initial conditions for them. They will be completely determined by the remaining renormalized quantities, and the flow equations of these will only be influenced via the anomalous dimensions.

Scalar Anomalous Dimension

As before, we start deriving the flow equation of $Z_{\varphi,k}$ by giving the projection rule onto the kinetic operator $(\partial_\mu \varphi)^2$:

$$Z_{\varphi,k} = \frac{\partial}{\partial p^2} \frac{\partial}{\partial \Delta\varphi(p)} \frac{\partial}{\partial \Delta\varphi(q)} \Gamma_k \Big|_{\substack{\Delta\varphi=\bar{\psi}=\psi=0 \\ p=q=0}} . \tag{3.28}$$

Here we are projecting with respect to $\Delta\varphi$, and not the full scalar field $\varphi = \varphi_{\mathrm{vev}} + \Delta\varphi$, since the excitation above the vacuum expectation value represents the relevant

dynamical degree of freedom. In the case were we have no vev there is evidently no difference between these two cases.
The flow equation is then, with Eq. (2.34), given by

$$\partial_t Z_{\varphi,k} = \frac{1}{2}\frac{\partial}{\partial p^2}\frac{\delta}{\delta\varphi(p)}\frac{\delta}{\delta\varphi(q)}\mathrm{STr}\left[\left(\partial_t R_k\right)\left(\Gamma_k^{(2)}+R_k\right)^{-1}\right]\Big|_{\substack{\Delta\varphi=\bar{\psi}=\psi=0\\ p=q=0}}. \tag{3.29}$$

As it was the case for the Yukawa coupling, we decompose $\left(\Gamma_k^{(2)}+R_k\right)$ into the propagator and field part, as shown in Eq. (3.20). We then look at the quadratic part in the expansion of the logarithm, since we are differentiating twice with respect to the field $\Delta\varphi$. The flow equation is then

$$\partial_t Z_{\varphi,k} = -\frac{1}{4}\frac{\partial}{\partial p^2}\frac{\delta}{\delta\varphi(p)}\frac{\delta}{\delta\varphi(q)}\mathrm{STr}\left[\tilde{\partial}_t\left\{\left(\Gamma_{k,0}^{(2)}+R_k\right)^{-1}\Delta\Gamma_k^{(2)}\right\}^2\right]\Big|_{\substack{\Delta\varphi=0\\ \bar{\psi}=\psi=0\\ p=q=0}}, \tag{3.30}$$

where we can ease the computation by setting the fermionic fields to zero right from the start since we are not taking derivatives with respect to them. After taking the trace over the internal space and performing the functional derivatives, we expand the result up to second order in p^2, since this is the relevant term when considering the projection rule. We arrive at

$$\begin{aligned}\partial_t Z_{\varphi,k} = \frac{1}{d}\int_p \tilde{\partial}_t\Bigg\{ & Z_{\varphi,k}^2\left(U_k'''(\varphi_{\mathrm{vev},k})\right)^2 p^2\left(\frac{\left(\frac{\partial}{\partial p^2}P(p)\right)}{\left[Z_{\varphi,k}P(p)+U_k''(\varphi_{\mathrm{vev},k})\right]^2}\right)^2 \\ +2d_\gamma\bar{h}_k^2\Bigg[& p^4\left(\frac{\partial}{\partial p^2}\frac{Z_{\psi,k}\left(1+r_{k,\mathrm{F}}(p)\right)}{Z_{\psi,k}^2P_{\mathrm{F}}(p)+\bar{h}_k^2\varphi_{\mathrm{vev},k}^2}\right)^2 - \bar{h}_k^2\varphi_{\mathrm{vev},k}p^2\left(\frac{\partial}{\partial p^2}\frac{1}{Z_{\psi,k}^2P_{\mathrm{F}}(p)+\bar{h}_k^2\varphi_{\mathrm{vev},k}^2}\right)^2\Bigg]\Bigg\}.\end{aligned} \tag{3.31}$$

As before, we introduce dimensionless, renormalized quantities and we get

$$\begin{aligned}\eta_{\varphi,k} = & 8\frac{v_d}{d}\Big\{\kappa_k\left[3u_k''(\kappa_k)+2\kappa_k u_k'''(\kappa_k)\right]^2 m_{4,0}^d\left(2\kappa_k u_k''(\kappa_k)+u_k'(\kappa_k),0;\eta_\varphi\right) \\ & + d_\gamma h_k^2\left[m_4^{(\mathrm{F})d}\left(2\kappa_k h_k^2;\eta_\psi\right)-2\kappa_k h_k^2 m_2^{(\mathrm{F})d}\left(2\kappa_k h_k^2;\eta_\psi\right)\right]\Big\}.\end{aligned} \tag{3.32}$$

The definitions of the threshold functions can be found in Appendix A and primes denote derivatives with respect to the dimensionless, renormalized field invariant $\tilde{\rho}$. The result agrees with that of [24].

Fermion Anomalous Dimension

For the fermionic anomalous dimension $\eta_{\psi,k}$ we repeat the same procedure as before. We project onto the fermionic kinetic term $\bar{\psi}\not{p}\psi$ via

$$Z_{\psi,k} = \frac{1}{4d_\gamma}\,\mathrm{tr}\,\gamma^\mu \frac{\partial}{\partial p^\mu}\frac{\overrightarrow{\delta}}{\delta\bar{\psi}(p)}\Gamma_k\frac{\overleftarrow{\delta}}{\delta\psi(q)}\bigg|_{\substack{\Delta\varphi=\bar{\psi}=\psi=0\\ p=q=0}}, \tag{3.33}$$

and using the Wetterich equation (2.34) we get the flow equation for $Z_{\psi,k}$ as

$$\begin{aligned}\partial_t Z_{\psi,k} &= \frac{1}{8d_\gamma}\,\mathrm{tr}\,\gamma^\mu \frac{\partial}{\partial p^\mu}\frac{\overrightarrow{\delta}}{\delta\bar{\psi}(p)}\mathrm{STr}\left[(\partial_t R_k)\left(\Gamma_k^{(2)}+R_k\right)^{-1}\right]\frac{\overleftarrow{\delta}}{\delta\psi(q)}\bigg|_{\substack{\Delta\varphi=\bar{\psi}=\psi=0\\ p=q=0}}\\ &= -\frac{1}{16d_\gamma}\,\mathrm{tr}\,\gamma^\mu \frac{\partial}{\partial p^\mu}\frac{\overrightarrow{\delta}}{\delta\bar{\psi}(p)}\mathrm{STr}\left[\tilde{\partial}_t\left\{\left(\Gamma_{k,0}^{(2)}+R_k\right)\Delta\Gamma_k^{(2)}\right\}^2\right]\frac{\overleftarrow{\delta}}{\delta\psi(q)}\bigg|_{\substack{\Delta\varphi=\bar{\psi}=\psi=0\\ p=q=0}}.\end{aligned} \tag{3.34}$$

In the second line we have again used the decomposition into propagator and field-dependent part (c.f. Eq. (3.20)), and we again keep only the quadratic part in the Taylor expansion, since we are differentiating with respect to fields twice. We can set the scalar excitation above the vev to zero right at the start, trace out the internal indices and perform the field derivatives. We then expand the result in the momentum p_μ and, regarding the projection rule, keeping only the term linear in p_μ we arrive at

$$\partial_t Z_{\psi,k} = \frac{2}{d}\bar{h}_k^2\int_p p^2\tilde{\partial}_t\left\{\frac{Z_{\psi,k}\left(1+r_{k,\mathrm{F}}(p)\right)}{Z_{\psi,k}^2 P_\mathrm{F}(p)+\bar{h}_k^2\varphi_{\mathrm{vev},k}^2}\frac{Z_{\varphi,k}\left(\frac{\partial}{\partial p^2}P(p)\right)}{\left[Z_{\varphi,k}P(p)+U_k'(\varphi_{\mathrm{vev},k})\right]^2}\right\}. \tag{3.35}$$

In dimensionless form, and all field strength renormalizations expressed through the anomalous dimensions, we have

$$\eta_{\psi,k} = 8h_k^2\frac{v_d}{d}m_{1,2}^{(\mathrm{FB})d}\left(2\kappa_k h_k^2, 2\kappa_k u_k''(\kappa_k)+u_k'(\kappa_k);\eta_\psi,\eta_\varphi\right), \tag{3.36}$$

where primes again denote derivatives with respect to $\tilde{\rho}$. The definitions of the threshold functions can also be found in Appendix A. As a cross check for these flow equations, we find the same results in the literature for the toy model studied here [22, 23].

4 Particle Masses from the FRG Flow

We now have all the necessary ingredients to study the renormalization group flow of our simple Yukawa-Higgs model. For this we set the dimension to $d = 4$. Furthermore we restrict ourselves to a quartic interaction in the scalar potential, i.e.

$$U_k\left(\varphi^2\right) = \frac{m_k^2}{2}\varphi^2 + \frac{\lambda_{2,k}}{24}\varphi^4. \tag{4.1}$$

The general case of a full potential has been studied in [22, 24]. For the purpose of the present work, our simple approximation is quantitatively adequate with an error on the $\mathcal{O}(10\%)$ level. If $m_k^2 > 0$, we are in the symmetric regime of the potential, characterized by a minimum situated at vanishing field $\phi = 0$. Looking at dimensionless couplings, we define the dimensionless mass term as $\lambda_{1,k} = m_k^2/k^2$ as in the previous section via running scale division. Should $\lambda_{1,k}$ become negative during our RG flow a minimum of the potential develops, such that $\phi \neq 0$. Owing to the $\mathbb{Z}_2$ symmetry of our model, there are two possible vacua in the latter case. We choose one of these as the ground state of our theory, giving rise to the spontaneous symmetry breaking (SSB) of said $\mathbb{Z}_2$ symmetry. In this phase we parametrize the potential by

$$U_k\left(\varphi^2\right) = \frac{\lambda_{2,k}}{6}\left(\rho_{0,k}^2 - \rho^2\right)^2, \tag{4.2}$$

where $\rho_{0,k}$ denotes the (scale-dependent) minimum of the potential. As for the scalar mass term we again look at dimensionless parameters and define $\kappa_k = \rho_{0,k}/k^2$. In the symmetry-broken regime we identify the masses by

$$v = Z_\varphi^{1/2}\langle\varphi\rangle, \qquad m_\mathrm{t} = hv, \qquad m_\mathrm{H} = \frac{1}{Z_\varphi}\frac{\partial^2 U}{\partial\varphi^2}\bigg|_{\varphi_0}, \tag{4.3}$$

here φ_0 denotes the minimum of the effective potential and all renormalized couplings are to be taken in the deep infrared. For our truncation this results in

$$v = \sqrt{2\kappa}k, \qquad m_\mathrm{t} = hv, \qquad m_\mathrm{H} = \sqrt{\frac{\lambda_2}{3}}v. \tag{4.4}$$

The flows of the two couplings $\lambda_{1,k}, \lambda_{2,k}$ in the symmetric, or $\lambda_{2,k}$ in the SSB phase, can be derived from Eq. (3.15) by projecting onto the respective coupling straightforwardly. Only for the minimum κ_k it is a little involved, since the reference configuration has a nonvanishing vacuum expectation value. Since κ_k is the minimum of the potential, we have

$$\partial_\rho u_k(\kappa_k) = 0. \tag{4.5}$$

Acting with a t derivative on both sides yields

$$\partial_\rho \partial_t v_k(\kappa_k) + \partial_\rho^2 v_k(\kappa_k)\, \partial_t \kappa_k = 0. \tag{4.6}$$

From this, the beta function for κ_k is easily obtained. We get

$$\partial_t \kappa_k = -\left.\frac{\partial_\rho \partial_t v_k(\rho)}{\partial_\rho^2 v_k(\rho)}\right|_{\rho=\kappa_k}. \tag{4.7}$$

For a given cutoff Λ the FRG equations map the bare parameters $m_\Lambda^2, \lambda_\Lambda$ and h_Λ to the physical quantities v, m_t and m_H. The only dimensionful parameter m_Λ^2 is tuned such that we get the correct vacuum expectation value of $v \simeq 246\,\mathrm{GeV}$, setting the scale in the infrared. Fixing m_Λ^2 is a numerical fine tuning problem, corresponding to the scale separation of Λ and electroweak scale in the standard model. We have to tune this value close to a partial fixed point in the β function of m^2 such that the dimensionful quantity in our model (m^2 in the symmetric, v in the broken regime) remains small over many scales, thus achieving the desired maximal separation of the UV scale Λ and the Fermi scale v. We then vary h_Λ until we get the right top mass of $m_\mathrm{t} \simeq 173\,\mathrm{GeV}$. Since we restrict ourselves to a φ^4 potential, λ_Λ is an arbitrary non-negative number to guarantee vacuum stability.
For a small scalar coupling λ_Λ at the cutoff, the flow usually starts in the symmetric regime. Near the electroweak scale fermionic fluctuations drive the system into the SSB regime, at $m_k^2 < 0$ we switch to the parametrization of the potential in the broken phase and continue with the SSB flow. A nonzero vev develops, giving rise to fermion mass. The modes start to decouple, freezing out the flow, i.e. all flow equations go to zero for $k \to 0$. In the case of a large bare scalar coupling λ_Λ, we already start in the broken regime, κ_Λ is already nonzero, albeit small. This minimum can remain small over long RG time until eventually it grows large again

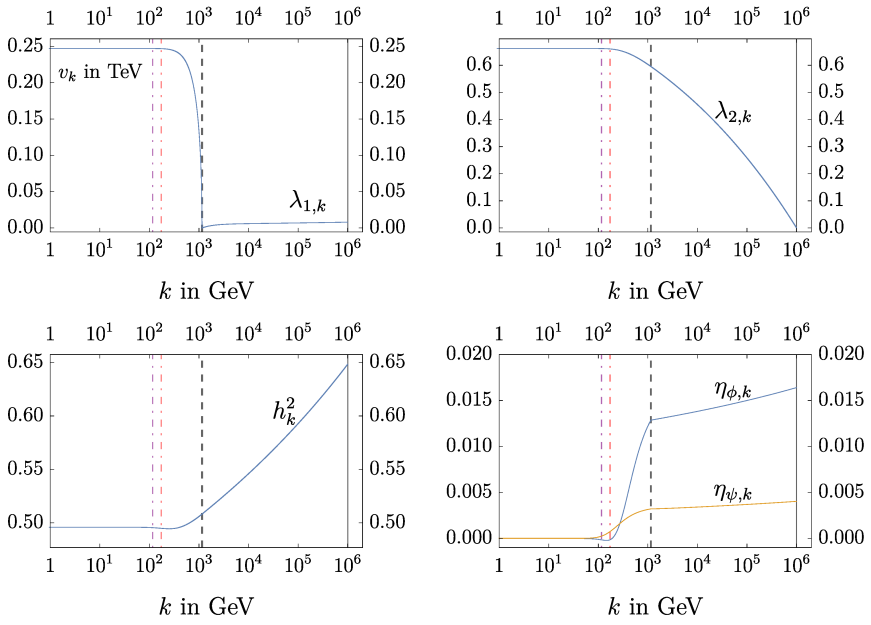

Figure 4.1.: FRG flow for a trajectory with $\Lambda = 10^6\,\mathrm{GeV}$ and $\lambda_{2,\Lambda} = 0$. h_Λ and $\lambda_{1,\Lambda}$ are tuned such that the flow ends in the broken regime with a vev of 246 GeV and $m_\mathrm{t} = 173\,\mathrm{GeV}$. At around 1 TeV (grey dashed line) the system transitions from the symmetric to the broken regime and we switch to the potential which expands around a nonzero vev κ_k. At the masses m_H (red dotted line) and m_t (purple dotted line) the modes decouple and the flow freezes out.

near the electroweak scale, implying the decoupling of all modes. An example flow is depicted in figure 4.1. We repeat this procedure for different initial values of λ_Λ while keeping $v \simeq 246\,\mathrm{GeV}$ and $m_\mathrm{t} \simeq 173\,\mathrm{GeV}$ fixed, obtaining a range of accessible Higgs masses from the flow. The upper bound arises from a Landau pole of the quartic coupling $\lambda_{2,\Lambda} \to \infty$ at a finite cutoff Λ. This behavior is also seen in perturbative calculations. The lower bound comes from vacuum stability arguments where $\lambda_{2,\Lambda} = 0$ at the cutoff and would turn negative for higher energies. While including higher order terms in the potential could cure this problem, the Yukawa coupling also diverges at finite energy, thus preventing the extension of this toy model to arbitrarily high cutoffs.
Having gained insight on the allowed Higgs masses for the measured value of $m_\mathrm{t} \simeq 173\,\mathrm{GeV}$, we then check the RG flows for other values of the top mass. For these calculations we keep the vacuum expectation value fixed at the standard model value of $v \simeq 246\,\mathrm{GeV}$. The resulting accessible parameter range is depicted in figure 4.2. For this analysis we started in the IR, solving the flow equations towards the UV.
The lower and upper bound approach each other at a fixed ratio of $m_\mathrm{H}/m_\mathrm{t}$, singling out a Higgs mass for a given m_t for which we separate the two scales of interest (the electroweak scale v and the cutoff Λ) maximally. This can be traced back to a fixed point in the RG flow of the composite coupling $\lambda_{2,k}/h_k^2$. As we can see in Figure 4.2 this maximal UV extension of the toy model can be increased by decreasing the top mass, and accordingly m_H. The cutoff Λ goes to infinity for m_t and $m_\mathrm{H} \to 0$, this however corresponds to a free scalar field and a free Dirac fermion which do not interact with each other. It is thus not possible to extend this model to arbitrarily high energies while still keeping to model interacting, which is known as the triviality problem.
When looking at the IR masses for fixed h_Λ and $\lambda_{2,\Lambda}$ while varying $\lambda_{1,\Lambda}$, we see that in the SYM regime there is no vacuum expectation value, and thus the top quark remains massless. The scalar field still has a mass which is just given by the operator $\frac{1}{2}m^2\varphi^2$. This is shown in figure 4.3, visualising the fine tuning problem necessary to separate the electroweak scale from the cutoff.
In the language of critical phenomena, v and m_t serve as an order parameter for a 2nd order quantum phase transition with $\delta\lambda_{1,\Lambda}$ corresponding to a control parameter that can be used to tune the system to criticality. From Fig. 4.3, it is obvious that the system has to be tuned very close to the phase transition in order to separate all physical mass scales from the cutoff scale, $m_\mathrm{t}, m_\mathrm{H}, v \ll \Lambda$. This is a manifestation of the fine-tuning/naturalness problem.

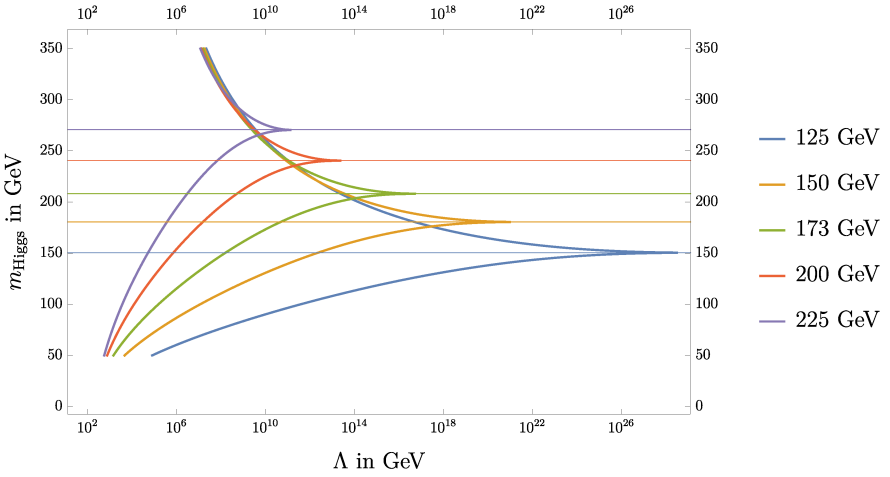

Figure 4.2.: Resulting upper and lower bounds for the Higgs masses for varying m_t while keeping the vev fixed at $v \simeq 246\,\mathrm{GeV}$. The upper bounds arise from a Landau pole in the quartic coupling $\lambda_{2,\Lambda}$ while the lower bounds come from demanding vacuum stability. These two bounds approach each other at a point of maximal UV extension of this toy model, giving a parameter set for which we can achieve maximal scale separation between the electroweak scale v and the cutoff Λ. This point is approached for a fixed ratio $m_\mathrm{H}/m_\mathrm{t}$ (solid lines of the appropriate color), which can be attributed to a fixed point in the RG flow of $\lambda_{2,k}/h_k^2$. For decreasing m_t, and thus also smaller m_H, the separation of the two aforementioned scales increases.

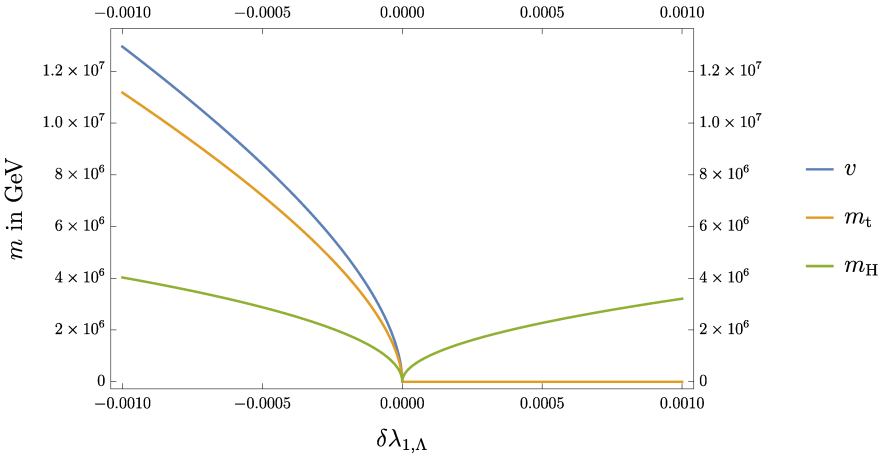

Figure 4.3.: Resulting masses in the IR for a cutoff of $\Lambda = 10^8\,\mathrm{GeV}$. The couplings h_Λ and $\lambda_{2,\Lambda}$ are kept fixed while the relevant coupling $\lambda_{1,\Lambda}$ gets varied. The fine tuning necessary to achieve a large separation between the cutoff and the electroweak scale (blue line) can be clearly seen, a small change in $\lambda_{1,\Lambda}$ will lead to a vacuum expectation value of $\mathcal{O}(\Lambda)$, resulting in a very heavy Higgs boson (green line) and top quark (orange line).

4.1. Fixed Ratio of Higgs/Top Mass for Maximal UV Extension

In the previous paragraph we found that for a fixed ratio of $m_{\mathrm{H}}/m_{\mathrm{t}}$, the cutoff can be separated from the electroweak scale maximally. This stems from a fixed point of the perturbative beta function of the ratio $\lambda_{2,k}/h_k^2$. Since this ratio is directly proportional to $m_{\mathrm{H}}^2/m_{\mathrm{t}}^2$, finding a fixed point in the perturbative beta functions gives us a relation between the two masses. We get the leading-order perturbative beta function of the composite coupling under consideration by setting the anomalous dimensions in the threshold functions to zero since these correspond to higher loop corrections. Furthermore we go to the deep Euclidean region where all masses are considered as small compared to the squared momenta or RG scales. In this approximation we can also set the involved mass term $\lambda_{1,k}$ to zero. Applying this to the flow equations derived in section 3 we get

$$\partial_t \left(\frac{\lambda_{2,k}}{h_k^2} \right) = \frac{h_k^2}{16\pi^2} \left(-48 - 2 \left(\frac{\lambda_{2,k}}{h_k^2} \right) + 3 \left(\frac{\lambda_{2,k}}{h_k^2} \right)^2 \right). \tag{4.8}$$

This equation is zero if the term in parentheses is equal to zero. We get the fixed point as

$$\frac{\lambda_{2,*}}{h_*^2} = \frac{1 + \sqrt{145}}{3}. \tag{4.9}$$

With the relation between Higgs and top mass we then arrive at

$$\frac{m_{\mathrm{H}}^2}{m_{\mathrm{t}}^2} = \frac{\lambda_{2,*}}{3h_*^2} \qquad \longleftrightarrow \qquad \frac{m_{\mathrm{H}}}{m_{\mathrm{t}}} = \frac{\sqrt{1 + \sqrt{145}}}{3} \tag{4.10}$$

which fits nicely to our data, although we used the perturbative beta function for the derivation of the fixed point, and not the full flow equation derived by the functional renormalization group.

5 Inclusion of Gauge Interactions

We now want to focus our attention on the transition from the symmetric regime to the broken phase (see Fig. 4.3). In particular we want to investigate the influence of gauge interactions on this phase transition.
In strongly interacting field theories like quantum chromodynamics we observe a phenomenon that high energy degrees of freedom (quarks and gluons) can vary substantially from the macroscopic degrees of freedom (fermionic bound states). These quark-antiquark bound states (mesons) and their properties are a manifestation of chiral symmetry breaking (χSB) at low momenta.

5.1. Quantum Chromodynamics

The fundamental theory describing strong interactions is called quantum chromodynamics (QCD), which is formulated as a non-abelian gauge theory based on the symmetry group SU(N_c), where in the case of QCD itself we have $N_\mathrm{c} = 3$. It is a theory consisting of N_f Dirac fermions transforming in the fundamental representation of SU(N_c), in the context of QCD called quarks, and $N_\mathrm{c}^2 - 1$ gauge bosons in the adjoint representation. The theory is defined via the microscopic action (already including a gauge-fixing term)

$$S_\mathrm{QCD} = \int_x \bar{\psi}_i^a \mathrm{i}\not{D}_{ij} \psi_j^a + \frac{1}{4} F_{\mu\nu}^z F_z^{\mu\nu} + \frac{(\partial_\mu A_z^\mu)^2}{2\xi}. \tag{5.1}$$

The quarks are taken to be massless and are described by the spinor fields $\bar{\psi}_i^a$ and ψ_i^a, where $a = 1, ..., N_\mathrm{f}$ denotes the quark flavor and $i = 1, ..., N_\mathrm{c}$ denotes the color index. The covariant derivative D_{ij}^μ in the fundamental representation couples quarks to the non-abelian gauge bosons $(A^\mu)_{ij}$ and is given by

$$D_{ij}^\mu = \partial^\mu \delta_{ij} - ig(A^\mu)_{ij}. \tag{5.2}$$

The gauge bosons A^μ_{ij} are $\mathfrak{su}(N_\mathrm{c})$ Lie algebra valued and can therefore be spanned by the $N_\mathrm{c}^2 - 1$ generators of the Lie algebra in the fundamental representation

$$(A^\mu)_{ij} = A^\mu_z (T^z)_{ij}. \tag{5.3}$$

The generators obey the Lie algebra

$$[T^x, T^y] = \mathrm{i} f^{xyz} T^z, \tag{5.4}$$

f^{xyz} denoting the structure constants of the Lie algebra $\mathfrak{su}(N_\mathrm{c})$. Here $x, y, z = 1, \cdots, N_\mathrm{c}^2 - 1$ denote adjoint color indices. The non-abelian field strength tensor is defined as the commutator of covariant derivatives

$$F_{\mu\nu} = \frac{1}{-\mathrm{i}g}[D_\mu, D_\nu] = \partial_\mu A_\nu - \partial_\nu A_\mu - \mathrm{i}g[A_\mu, A_\nu] = F^z_{\mu\nu} T^z, \tag{5.5}$$

where we again have expanded the field strength tensor by means of the Lie algebra generators. The QCD action supports a chiral symmetry, which refers to the symmetry of independent unitary flavor transformations of the left- and right-handed components of Dirac fermions. We can project onto the left- and right-handed parts by applying the projection operators

$$P_{\mathrm{R/L}} = \frac{1}{2}\left(1 \pm \gamma_5\right). \tag{5.6}$$

One feature of QCD is asymptotic freedom, implying that perturbative calculations are only valid in the high energy region where the corresponding gauge coupling is small. If we turn towards lower energies, the coupling strength increases as was first shown by Gross, Wilczek and Politzer [25, 26]. This invalidates perturbation theory in the infrared and we have to turn towards non-perturbative methods and use effective field theoretic descriptions to access the low energy effects, starting roughly at $\Lambda = \mathcal{O}(1\,\mathrm{GeV})$. The scale at which perturbative calculations show a Landau pole in the gauge coupling is called Λ_QCD, and this is the characteristic scale of QCD.

Owing to quantum fluctuations (see Fig. 5.1), the fermion-gluon interactions induce new effective four-fermion vertices. We therefore introduce the effective average action (see [27])

$$\begin{aligned}\Gamma_k = &\int_x \bar\psi^a_i (\mathrm{i} Z_\psi \partial\!\!\!/ \delta_{ij} + \bar g A\!\!\!/_{ij}) \psi^a_j + \frac{Z_F}{4} F^z_{\mu\nu} F_z^{\mu\nu} + \frac{(\partial_\mu A^\mu_z)^2}{2\xi} \\ &+ \frac{1}{2}\Big[\bar\lambda_-(\mathrm{V}-\mathrm{A}) + \bar\lambda_+(\mathrm{V}+\mathrm{A}) + \bar\lambda_\sigma(\mathrm{S}-\mathrm{P}) + \bar\lambda_{\mathrm{VA}}[2(\mathrm{V}-\mathrm{A})^{\mathrm{adj}} + (1/N_\mathrm{c})(\mathrm{V}-\mathrm{A})]\Big].\end{aligned} \tag{5.7}$$

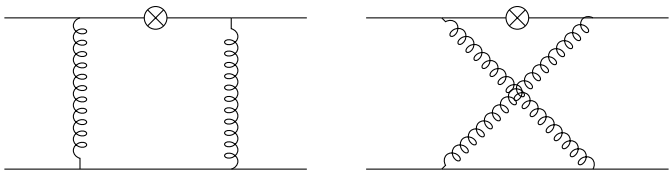

Figure 5.1.: The effective four-fermion interactions are generated within fundamental QCD (cf. Eq. (5.1)) through quark-gluon interactions. Even when we set the four-fermion couplings $\bar{\lambda}_i$ to zero at one scale, quantum fluctuations will generate these effective vertices at different scales.

The different four-fermion interactions introduced here form a complete basis, meaning that any other point-like fermionic self interaction can be decomposed into these basis elements by means of Fierz transformations. They can be classified by their color and flavor structure, with

$$\begin{aligned} (\mathrm{V}-\mathrm{A}) &= (\bar{\psi}\gamma_\mu\psi)^2 + (\bar{\psi}\gamma_\mu\gamma_5\psi)^2 \\ (\mathrm{V}+\mathrm{A}) &= (\bar{\psi}\gamma_\mu\psi)^2 - (\bar{\psi}\gamma_\mu\gamma_5\psi)^2 \end{aligned} \tag{5.8}$$

being color and flavor singlets, where the respective indices (i, j) and (a, b) are pairwise contracted, $(\bar{\psi}\psi) = (\bar{\psi}_i^a\psi_i^a)$. The two operators

$$\begin{aligned} (\mathrm{S}-\mathrm{P}) &= (\bar{\psi}_i^a\psi_i^b)^2 - (\bar{\psi}_i^a\gamma_5\psi_i^b)^2 \\ (\mathrm{V}-\mathrm{A})^{\mathrm{adj}} &= (\bar{\psi}_i^a\gamma_\mu(T^z)_{ij}\psi_j^a)^2 + (\bar{\psi}_i^a\gamma_\mu\gamma_5(T^z)_{ij}\psi_j^a)^2 \end{aligned} \tag{5.9}$$

have non-trivial flavor or color structure. Here we write $(\bar{\psi}^a\psi^b)^2 = \bar{\psi}^a\psi^b\bar{\psi}^b\psi^a$ for short, $(T^z)_{ij}$ again denotes the generators of the gauge group in the fundamental representation. These four-fermion interactions are controlled by their fixed-point structure [27]. A fixed point corresponds to a simultaneous zero of all β functions in the theory. The flow equations for these (dimensionless, renormalized) four-fermion couplings

$$\lambda_i = \frac{k^2\bar{\lambda}_i}{Z_\psi^2} \tag{5.10}$$

for fixed gauge coupling g^2 take the form [27]

$$\partial_t\lambda_i = (d-2)\lambda_i + \lambda_k A_i^{kl}\lambda_l, \tag{5.11}$$

where A_i^{kl} are constant matrices, symmetric in the upper indices. These β functions correspond to parabolas in the space of all λ_i, each having exactly two fixed-point solutions. Since we have four fermionic couplings, we expect this system to have 16

fixed points. For vanishing gauge coupling we see 15 interacting fixed points and one IR attractive non interacting (Gaussian) one. With increasing g^2 these parabolas are shifting upwards and, at a critical gauge coupling strength $\alpha_{\mathrm{cr}} = g_{\mathrm{cr}}^2/4\pi$, one interacting fixed point annihilates with the (for $g^2 = 0$) Gaussian one. For a schematic plot of such a parabola loosing its roots, see Figure 5.2 in the next section. An algebraic inspection of Eq. (5.11) reveals that the fixed point annihilating with the Gaussian one at $\alpha_{\mathrm{cr}} \approx 0.84$ is dominated by a large scalar-pseudoscalar four-fermion coupling λ_σ and we find

$$(\lambda_\sigma, \lambda_{\mathrm{VA}}, \lambda_+, \lambda_-)|_{\alpha_{\mathrm{cr}}} \approx (5.898, -0.433, 0.003, 0.454). \tag{5.12}$$

At that point the couplings are no longer controlled by these fixed points and they start to grow large. Eventually the couplings diverge, signaling the onset of chiral symmetry breaking, as elucidated in the next section. As indicated by the comparatively large value of λ_σ at the critical value of the gauge coupling (see Eq. (5.12)), the chiral symmetry breaking is driven by the scalar-pseudoscalar channel.
For this reason, as well as since the chiral condensate originating from this operator shares some quantum numbers with the Higgs field and thus also implying Dirac masses for the fermions in the χSB phase, we restrict ourselves to just the $(\mathrm{S}-\mathrm{P})$ channel in this work.

5.2. Partial Bosonization

To consistently connect the microscopic theory with the macroscopic one, we use the Hubbard-Stratonovich transformation to model the transition from fermions to bosons. We start with the QCD action motivated in the previous section with the additional scalar-pseudoscalar four-fermion interaction, which is similar to the gauged Nambu–Jona-Lasinio (NJL) model, containing N_{f} fermions defined by the action

$$S_{\mathrm{F}} = \int_x \bar{\psi}^a \mathrm{i}\not{\partial}\psi^a + \frac{1}{2}\bar{\lambda}_\sigma \left[(\bar{\psi}^a \psi^b)^2 - \left(\bar{\psi}^a \gamma_5 \psi^b\right)^2 \right]. \tag{5.13}$$

Here we have suppressed the gauge sector for brevity, since it has no influence on the following arguments. This model has an $\mathrm{SU}(N_{\mathrm{f}})_{\mathrm{R}} \times \mathrm{SU}(N_{\mathrm{f}})_{\mathrm{L}}$ symmetry, containing the chiral symmetry, which (perturbatively) protects the fermions against acquiring a mass through fluctuations.
We can then introduce a mixed bosonic and fermionic theory

$$S_{\mathrm{FB}} = \int_x \bar{\psi}^a \mathrm{i}\not{\partial}\psi^a + m^2 \varphi^{ab}\varphi^{*ab} + \mathrm{i}\bar{h}\bar{\psi}^a \left[P_{\mathrm{R}}\varphi^{ab} + P_{\mathrm{L}}\varphi^{*ba} \right] \psi^b. \tag{5.14}$$

These two models are equivalent, since we can write

$$S_{\mathrm{FB}} = \int_x \bar{\psi}^a \mathrm{i}\partial\!\!\!/ \psi^a + \left[(\varphi^{*ab} + \mathrm{i}\frac{\bar{h}}{m^2}\bar{\psi}^a P_{\mathrm{R}}\psi^b) m^2 (\varphi^{ab} + \mathrm{i}\frac{\bar{h}}{m^2}\bar{\psi}^b P_{\mathrm{L}}\psi^a) \right] + \frac{\bar{h}^2}{m^2}\bar{\psi}^a P_{\mathrm{R}}\psi^b \bar{\psi}^b P_{\mathrm{L}}\psi^a. \tag{5.15}$$

Using

$$\bar{\psi}^a P_{\mathrm{R}}\psi^b \bar{\psi}^b P_{\mathrm{L}}\psi^a = \frac{1}{4}\left[(\bar{\psi}^a\psi^b)^2 - (\bar{\psi}^a\gamma_5\psi^b)^2 \right] \tag{5.16}$$

and choosing

$$m^2 = \frac{\bar{h}^2}{2\bar{\lambda}_\sigma}, \tag{5.17}$$

we see that the partition functions of both models agree up to an irrelevant constant

$$\int \mathcal{D}\varphi \mathcal{D}\varphi^* \mathrm{e}^{-S_{\mathrm{FB}}} = \mathcal{N}\mathrm{e}^{-S_{\mathrm{F}}}, \tag{5.18}$$

since the part in brackets in Eq. (5.15) just gives a Gaussian integral, which is a pure number being absorbed in the normalization factor. This fermionic pairing can also be seen in the classical equations of motion

$$\varphi^{ab} = -\mathrm{i}\frac{\bar{h}}{m^2}\bar{\psi}^b P_{\mathrm{L}}\psi^a, \qquad \varphi^{*ab} = -\mathrm{i}\frac{\bar{h}}{m^2}\bar{\psi}^a P_{\mathrm{R}}\psi^b. \tag{5.19}$$

We see that we can choose $\lambda_{\sigma,\Lambda} = 0$ for a certain choice of the other parameters h_Λ^2 and m_Λ^2 at a UV scale Λ, but as already said in the previous section, quantum fluctuations will nevertheless generate a non-zero effective four-fermion coupling with only fundamental QCD interactions taken into account (see Fig. 5.1). This is captured in the flow equation of said coupling, and we write it as [27]

$$\begin{aligned}
\partial_t \bar{\lambda}_\sigma &= \frac{Z_\psi^2}{k^2}\left[\beta_{\lambda_\sigma}^{g^4} g^4 + \beta_{\lambda_\sigma}^{g^2h^2} g^2 h^2 \right], \\
\beta_{\lambda_\sigma}^{g^4} &= -\frac{1}{4}\frac{9N_{\mathrm{c}}^2 - 24}{N_{\mathrm{c}}} v_d l_{1,2}^{(\mathrm{FB})d}\left(0, 0; \eta_\psi, \eta_{\mathrm{F}}\right), \\
\beta_{\lambda_\sigma}^{g^2h^2} &= \frac{48}{N_{\mathrm{c}}} v_d l_{1,1,1}^{(\mathrm{FBB})d}\left(0, m^2 k^{-2} Z_\varphi^{-1}, 0; \eta_\psi, \eta_\varphi, \eta_{\mathrm{F}}\right).
\end{aligned}$$

The definition of the threshold function $l_{1,1,1}^{(\mathrm{FBB})d}$ can be found in Appendix A. In order to cope with this and keep the four-fermion coupling fixed to zero at all times, we promote the Hubbard-Stratonovich field to be scale dependent. The flow equation then gets an additional contribution [17]

$$\partial_t \Gamma_k[\varphi_k]|_{\varphi_k} = \partial_t \Gamma_k[\varphi_k] - \int \frac{\delta\Gamma_k[\varphi_k]}{\delta\varphi_k}\partial_t\varphi_k, \tag{5.20}$$

where the first part is the usual term $\sim \mathrm{STr}\, G_k \partial_t R_k$ and the second part takes the scale dependence of the fields into account. This approach follows from an approximation to an exact equation [28] where the neglected terms are parametrically suppressed for the present application [17].
We choose the ansatz

$$\begin{aligned} \partial_t \varphi_k^{ab}(q) &= -\mathrm{i}\bar{\psi}^b P_\mathrm{L} \psi^a(q) \partial_t \alpha_k(q) + \varphi^{ab} \partial_t \beta_k(q) \\ \partial_t \varphi^{*ab}(q) &= -\mathrm{i}\bar{\psi}^a P_\mathrm{R} \psi^b(-q) \partial_t \alpha_k(q) + \varphi^{*ab} \partial_t \beta_k(q), \end{aligned} \tag{5.21}$$

α and β being a priori arbitrary functions to be defined below. These scale dependencies, together with the modified flow equation (5.20), yield the beta functions for the couplings

$$\begin{aligned} \partial_t Z_\varphi q^2 + \partial_t m^2 &= \partial_t m^2 \Big|_{\varphi_k} + 2(Z_\varphi q^2 + m^2) \partial_t \beta_k(q), \\ \partial_t \bar{h} &= \partial_t \bar{h} \Big|_{\varphi_k} + (Z_\varphi q^2 + m^2) \partial_t \alpha_k(q) + \bar{h} \partial_t \beta_k(q), \\ \partial_t \bar{\lambda}_\sigma &= \partial_t \bar{\lambda}_\sigma \Big|_{\varphi_k} - \bar{h} \partial_t \alpha_k(q). \end{aligned} \tag{5.22}$$

From this so-called dynamical bosonization, together with our goal of vanishing four-fermion coupling on all scales, we can immediately identify the function $\partial_t \alpha_k(q)$ as

$$\partial_t \alpha_k(q) = \frac{1}{\bar{h}} \partial_t \bar{\lambda}_\sigma(q). \tag{5.23}$$

Furthermore we want to achieve a momentum-independent Yukawa coupling $\bar{h}$, such that the IR observables like fermion masses are independent of the involved momenta, and a momentum-independent scalar field renormalization Z_φ to be self consistent within our truncation. With these goals in mind, we can uniquely determine the latter of the two functions [29] and we get

$$\partial_t \beta_k(q) = -\frac{Z_\varphi q^2 + m^2}{\bar{h}^2} \partial_t \bar{\lambda}_\sigma(q^2) + \frac{1}{Z_\varphi k^2 \bar{h}^2} \left[(Z_\varphi k^2 + m^2)^2 \partial_t \bar{\lambda}_\sigma(k^2) - m^4 \partial_t \bar{\lambda}_\sigma(0) \right]. \tag{5.24}$$

Through these functions the gauge sector which previously only affected the fermionic self interaction now influences the scalar potential as well as the Yukawa interaction. Like in the fully fermionic theory, at a critical value of the gauge coupling $\alpha_\star$, we will enter the chiral symmetry-breaking regime. This can be seen clearly when looking at the dimensionless composite coupling

$$\tilde{\epsilon} \coloneqq \frac{m^2}{h^2 k^2} \tag{5.25}$$

together with its flow equation

$$\partial_t \tilde{\epsilon} = -2\tilde{\epsilon} + A + Bg^2\tilde{\epsilon} - 2\tilde{\epsilon}\frac{m^2}{h}\partial_t \alpha_k = -2\tilde{\epsilon} + A + Bg^2\tilde{\epsilon} + 2Cg^4\tilde{\epsilon}^2. \tag{5.26}$$

For the last equality we have neglected the last part of Eq. (5.20) $\sim h^2 g^2$ since this gives a subleading contribution to the flow. We also note that this flow equation is independent of the choice of $\partial\beta_k$. The constants A, B and C are all positive quantities [17] and the last term comes directly from the bosonization of the four-fermion interaction. Thus the RHS of the flow equation looks like a parabola which is lifted for increasing gauge coupling g, as can be seen in Fig. 5.2. At the critical gauge coupling the two roots of the parabola (fixed points) are destabilized and we run into the chiral symmetry-breaking regime, characterized by a negative m^2 and therefore negative $\tilde{\epsilon}$.

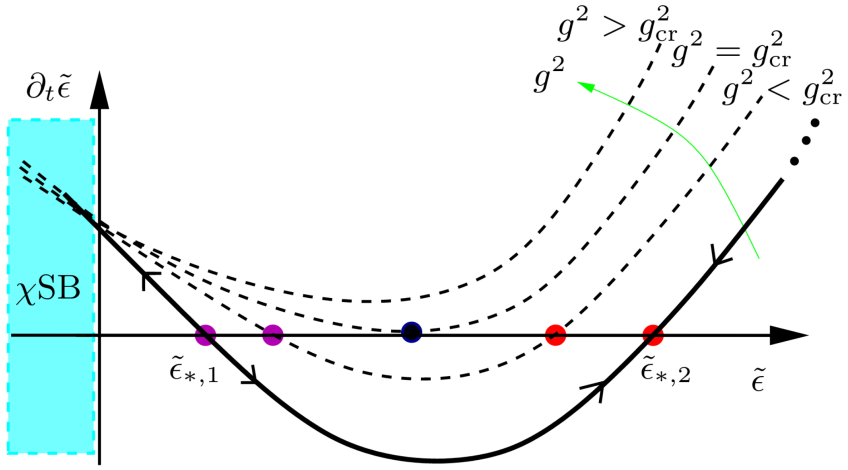

Figure 5.2.: Schematic plot of the flow equation Eq. (5.26) of the composite coupling $\tilde{\epsilon}$. The arrows are pointing towards the IR. At small gauge couplings g^2 this coupling is controlled by its fixed point $\tilde{\epsilon}_{*,2}$ Increasing the gauge coupling lifts the parabola upwards and at a critical coupling g^2_{cr} the two fixed points annihilate. The flow is then no longer controlled by the fixed-point structure, and we rapidly run into the chiral symmerty-breaking regime, characterized by negative $\tilde{\epsilon}$. Figure taken from [17].

5.3. Full Model

With these tools at hand, we can now turn to the model of interest in the second part of this work. We look at a chiral Higgs-top-bottom model [30,31], comparable to the

very simple toy model we started with, containing two Dirac fermions representing the top and bottom quark as well as a complex scalar field

$$\phi = \frac{1}{\sqrt{2}} \begin{pmatrix} \phi_1 + \mathrm{i}\phi_2 \\ \phi_4 + \mathrm{i}\phi_3 \end{pmatrix} \tag{5.27}$$

representing the Higgs field. This couples to the two quarks of interest which we split into their left and right handed components and write

$$\psi_{\mathrm{L}} = \begin{pmatrix} t_{\mathrm{L}} \\ b_{\mathrm{L}} \end{pmatrix}, \qquad t_{\mathrm{R}}, \qquad b_{\mathrm{R}}. \tag{5.28}$$

We then introduce gauge interactions and two more generations of quarks for a total of six quarks in this model in order to have a gauge sector comparable to the standard model. As seen in Section 5.1, this in turn generates four-fermion interactions and, focusing on the scalar-pseudoscalar channel, we then partially bosonize said interaction. Through the Hubbard-Stratonovich transformation we end up with an additional complex scalar matrix field φ^{ab} coupled to all fermions through a chiral Yukawa interaction. With all this in mind, we arrive at the effective average action

$$\begin{aligned} \Gamma_k = \int_x \Big[& Z_\phi |\partial_\mu \phi|^2 + U_k(\rho) + Z_\varphi \partial_\mu \varphi^{ab} \partial^\mu \varphi^{*ab} + V_k\left(\rho_{\mathrm{M}}, \tau\right) + \frac{Z_{\mathrm{F}}}{4} F^{z\mu\nu} F^z_{\mu\nu} + \frac{(\partial_\mu A^\mu_z)}{2\xi} \\ & + \bar{\psi}^a_i \left(Z^a_\psi \mathrm{i} \not{\partial} \delta_{ij} + \bar{g} \not{A}_{ij} \right) \psi^a_j + \mathrm{i}\bar{h}_{\mathrm{b}} \left(\bar{\psi}_{\mathrm{L}} \phi b_{\mathrm{R}} + \bar{b}_{\mathrm{R}} \phi^\dagger \psi_{\mathrm{L}} \right) + \mathrm{i}\bar{h}_{\mathrm{t}} \left(\bar{\psi}_{\mathrm{L}} \phi_{\mathcal{C}} t_{\mathrm{R}} + \bar{t}_{\mathrm{R}} \phi^\dagger_{\mathcal{C}} \psi_{\mathrm{L}} \right) \\ & + \mathrm{i}\bar{h} \bar{\psi}^a_i \left(P_{\mathrm{R}} \varphi^{ab} + P_{\mathrm{L}} \varphi^{*ba} \right) \psi^b_i \Big]. \end{aligned} \tag{5.29}$$

$Z^a_\psi = \left(Z^{\mathrm{t}}_\psi, Z^{\mathrm{b}}_\psi, Z_\psi, \cdots, Z_\psi \right)$ denote the wave function renormalizations for the top, the bottom and the $N_{\mathrm{f}} - 2$ remaining quarks respectively, Z_φ and Z_ϕ the ones of the scalar fields. $\phi_{\mathcal{C}} = \mathrm{i}\sigma_2 \phi^*$ with σ_2 being the second Pauli matrix is the charge conjugated scalar field. $\bar{h}_{\mathrm{t}}$ and $\bar{h}_{\mathrm{b}}$ are the bare Yukawa couplings for the top and bottom quark, while $\bar{h}$ is the Yukawa coupling originating from the Hubbard-Stratonovich transformation.
The action Eq. (5.29) is invariant under the global $\mathrm{SU}(2)_{\mathrm{L}}$ symmetry transformations

$$\phi \to \mathrm{e}^{\mathrm{i}\alpha_i \frac{\sigma^i}{2}} \phi, \quad \psi_{\mathrm{L}} \to \mathrm{e}^{\mathrm{i}\alpha_i \frac{\sigma^i}{2}} \psi_{\mathrm{L}}, \quad t_{\mathrm{R}} \to t_{\mathrm{R}}, \quad b_{\mathrm{R}} \to b_{\mathrm{R}}, \tag{5.30}$$

where σ^i are the Pauli matrices acting on the SU(2) doublet structure. By means of Eq. (5.19) the matrix field also transforms under this transformation

$$P_3 \varphi \to \mathrm{e}^{\mathrm{i}\alpha_i \frac{\sigma^i}{2}} P_3 \varphi. \tag{5.31}$$

Here P_3 denotes the projector onto the third generation of quarks, namely the top-bottom sector of the meson field. The symmetry $\mathrm{SU}(2)_\mathrm{R}$ is explicitly broken by the fact that h_t is different from h_b. Furthermore the action is invariant under $\mathrm{SU}(4)_\mathrm{L}\times\mathrm{SU}(4)_\mathrm{R}$ transformations acting on the first two quark generations and, as before, on the meson field

$$\begin{aligned}
\mathrm{L}: &\quad \psi_\mathrm{L} \to \mathrm{e}^{\mathrm{i}\alpha_i T^i}\psi_\mathrm{L}, \quad P_{12}\varphi \to \mathrm{e}^{\mathrm{i}\alpha_i T^i}P_{12}\varphi, \quad \psi_\mathrm{R} \to \psi_\mathrm{R}, \quad P_3\varphi \to P_3\varphi, \\
\mathrm{R}: &\quad \psi_\mathrm{R} \to \mathrm{e}^{\mathrm{i}\alpha_i T^i}\psi_\mathrm{R}, \quad P_{12}\varphi \to P_{12}\varphi\mathrm{e}^{-\mathrm{i}\alpha_i T^i}, \quad \psi_\mathrm{L} \to \psi_\mathrm{L}, \quad P_3\varphi \to P_3\varphi.
\end{aligned} \tag{5.32}$$

Here T^i denote the generators of SU(4), P_{12} is the projector in the first two quark generations in the matrix field, and $\psi_{\mathrm{L/R}}$ denotes only the first two quark generations.

Scalar Potentials

For both scalar potentials U_k and V_k we consider quartic approximations. In case of the Higgs scalar potential, which is a function of the field invariant $\bar{\rho} = \phi^\dagger\phi$, this means the function has the form

$$U_k(\bar{\rho}) = m^2\bar{\rho} + \frac{1}{2}\bar{\lambda}_\phi(\bar{\rho})^2. \tag{5.33}$$

m^2 denotes the scalar mass, while $\bar{\lambda}_\phi$ is the coupling associated with the scalar self interaction. Spontaneous symmetry breaking of $\mathrm{SU}(2)_\mathrm{L}$ occurs when this potential develops a nonvanishing minimum $\bar{\rho}_0$, thus the scalar field has a nonzero vev $\phi \to v$. We choose our fields in such a way that this happens in the real part of the second component of ϕ

$$\phi_0 = \frac{1}{\sqrt{2}}\begin{pmatrix}0\\ v\end{pmatrix}, \tag{5.34}$$

such that the top and bottom quark acquire Dirac masses through their Yukawa interactions

$$\mathrm{i}\bar{h}_\mathrm{t}\left(\bar{\psi}_\mathrm{L}\phi_\mathcal{C}t_\mathrm{R} + \bar{t}_\mathrm{R}\phi_\mathcal{C}^\dagger\psi_\mathrm{L}\right) \to \mathrm{i}\frac{\bar{h}_\mathrm{t}}{\sqrt{2}}v\left(\bar{t}_\mathrm{L}t_\mathrm{R} + \bar{t}_\mathrm{R}t_\mathrm{L}\right) + \text{fluctuations}, \tag{5.35}$$

and analogously for the bottom quark. These masses, as well as the Higgs mass, can then be expressed through that vev and the renormalized Yukawa couplings

$$\begin{aligned}
v &= \sqrt{Z_\phi\bar{\rho}_0}, & m_\mathrm{t}^2 &= \frac{1}{2}v^2h_\mathrm{t}^2, \\
m_\mathrm{H}^2 &= v^2\frac{U''(\bar{\rho}_0)}{Z_\phi^2}, & m_\mathrm{b}^2 &= \frac{1}{2}v^2h_\mathrm{b}^2,
\end{aligned} \tag{5.36}$$

the definition of the renormalized quantities can be found below.
The scalar potential of the Hubbard-Stratonovich field (meson potential) is chosen to be a function of the two invariants

$$\begin{aligned}\bar{\rho}_{\mathrm{M}} &= \frac{1}{2}\,\mathrm{tr}\Big(\varphi^{\dagger}\varphi\Big) \\ \bar{\tau} &= \frac{1}{2}\,\mathrm{tr}\bigg(\frac{1}{2}\varphi^{\dagger}\varphi - \frac{\bar{\rho}_{\mathrm{M}}}{2N_{\mathrm{f}}}\bigg)^{2},\end{aligned} \tag{5.37}$$

with the dependence on higher invariants present for $N_{\mathrm{f}} \geq 3$ neglected, owing to our quartic approximation. The meson potential with these invariants up to order φ^4 then reads

$$V_k(\bar{\rho}_{\mathrm{M}}, \tau) = m_{\mathrm{M}}^2 \bar{\rho}_{\mathrm{M}} + \frac{1}{2}\bar{\lambda}_1 \bar{\rho}_{\mathrm{M}}^2 + \bar{\lambda}_2 \bar{\tau}. \tag{5.38}$$

Spontaneous chiral symmetry breaking occurs, as in the case of the Higgs potential, when the minimum is at nonzero field value. We choose a diagonal vacuum configuration

$$\varphi_0 = \begin{pmatrix} \sigma_0 & & & \\ & \sigma_0 & & \\ & & \ddots & \\ & & & \sigma_0 \end{pmatrix}, \tag{5.39}$$

meaning all quarks acquire the same mass through chiral symmetry breaking. This corresponds to breaking the full $\mathrm{SU}(N_{\mathrm{f}})_{\mathrm{L}}\times\mathrm{SU}(N_{\mathrm{f}})_{\mathrm{R}}$ (which is an exact symmetry only for $h_{\mathrm{t}} = h_{\mathrm{b}} = 0$) down to its diagonal subgroup, with a residual vector-like $\mathrm{SU}(N_{\mathrm{f}})$ flavor symmetry. In the symmetric regime we choose our vacuum state to be $(\bar{\rho}_{\mathrm{M}}, \bar{\tau}) = (0, 0)$, while in the χSB phase we have $(\bar{\rho}_{\mathrm{M}}, \bar{\tau}) = (\bar{\rho}_{\mathrm{M}}, 0)$. With these choices we have N_{f} eigenvalues of the matrix $\varphi^{\dagger}\varphi$ given by 0 and $\frac{1}{N_{\mathrm{f}}}\rho_{\mathrm{M}}$ in the symmetric and χSB regime, respectively, and the scalar mass spectrum presented in Table 5.1. While in the symmetric regime there are $2N_{\mathrm{f}}^2$ scalar fields with mass V' and the fermions do not gain any mass, in the case of chiral symmetry breaking our spectrum enlarges, with N_{f}^2 scalar fields being massless due to Goldstone's theorem, $N_{\mathrm{f}}^2 - 1$ having squared mass equal to $\bar{\rho}_{\mathrm{M}}\bar{\lambda}_2/N_{\mathrm{f}}$ and one radial mode with squared mass $2\bar{\rho}_{\mathrm{M}}\bar{\lambda}_1$. Out of these N_{f}^2 Goldstone bosons, $N_{\mathrm{f}}^2 - 1$ come from the breaking of $\mathrm{SU}(N_{\mathrm{f}})_{\mathrm{L}}\times\mathrm{SU}(N_{\mathrm{f}})_{\mathrm{R}}$ to $\mathrm{SU}(N_{\mathrm{f}})_{\mathrm{V}}$, and one comes from the breaking of the $\mathrm{U}(1)_{\mathrm{A}}$ symmetry present in the current truncation of the model. Contributions from the axial anomaly are ignored in our study as the anomaly is not relevant for the top-Higgs sector. Since some components of the two scalar fields share the same quantum numbers χSB also induces a breaking of the $\mathrm{SU}(2)_{\mathrm{L}}$ symmetry. For a first glance at the system we will model this by shifting the Higgs vev by the meson vev,

Eigenvalue	Degeneracy
V'	N_f^2
$V' + \frac{\bar{\lambda}_2}{N_\mathrm{f}}\bar{\rho}_\mathrm{M}$	$N_\mathrm{f}^2 - 1$
$V' + 2\bar{\rho}_\mathrm{M}\bar{\lambda}_1$	1

Table 5.1.: Meson mass spectrum for the potential given in Eq. (5.38). Primes denote derivatives with respect to the field invariant $\bar{\rho}_\mathrm{M}$. The eigenvalues agree with those given in [32] and those given in [33] upon the replacement $\bar{\lambda}_2/N_\mathrm{f} \to \bar{\lambda}_2$.

$\rho \to \rho + \rho_\mathrm{M}$. The top and bottom quark in this case obtain a squared mass equal to $\frac{1}{2}h_{\mathrm{t/b}}^2\rho_\mathrm{M} + \bar{\rho}_\mathrm{M}h^2/N_\mathrm{f}$.

Flow Equations for the Full Model

Using this truncation in the Wetterich equation yields the β functions for the respective couplings as well as the wave function renormalizations of the fields for the given model. The latter will be encoded in the anomalous dimensions,

$$\eta_i = -\partial_t \log(Z_i), \tag{5.40}$$

i labeling the respective field. As done in the first model, it is useful to define dimensionless renormalized quantities as

$$\begin{aligned}
\rho &= Z_\phi k^{2-d}\bar{\rho}, & \epsilon &= Z_\phi^{-1}k^{-2}m^2, & \lambda_\phi &= Z_\phi^{-2}k^{d-4}\bar{\lambda}_\phi,\\
\rho_\mathrm{M} &= Z_\varphi k^{2-d}\bar{\rho}_\mathrm{M}, & \tau &= Z_\varphi^2 k^{4-2d}\bar{\tau}, & \epsilon_\mathrm{M} &= Z_\varphi^{-1}k^{-2}m_\mathrm{M}^2,\\
\lambda_1 &= Z_\varphi^{-2}k^{d-4}\bar{\lambda}_1, & \lambda_2 &= Z_\varphi^{-2}k^{d-4}\bar{\lambda}_2, & h_\mathrm{t}^2 &= Z_\phi^{-1}Z_\mathrm{L}^{-1}{Z_\mathrm{R}^\mathrm{t}}^{-1}\bar{h}_\mathrm{t}^2,\\
h_\mathrm{b}^2 &= Z_\phi^{-1}Z_\mathrm{L}^{-1}{Z_\mathrm{R}^\mathrm{b}}^{-1}\bar{h}_\mathrm{b}^2, & h^2 &= Z_\psi^{-2}Z_\varphi^{-1}k^{d-4}\bar{h}^2, & g^2 &= Z_\mathrm{F}^{-1}k^{d-4}\bar{g}^2.
\end{aligned} \tag{5.41}$$

The flow equation for the (dimensionless) Higgs scalar potential $u_k = k^{-d}U_k$ is then given by

$$\begin{aligned}
\partial_t u = &- du + (d - 2 + \eta_\phi)\rho u' + v_d\left(3l_0^d\left(u';\eta_\phi\right) + l_0^d\left(u' + 2\rho u'';\eta_\phi\right)\right)\\
&- d_\gamma N_\mathrm{c} v_d\left(l_0^{(\mathrm{F})d}\left(h_\mathrm{t}^2\rho + \frac{1}{N_\mathrm{f}}h^2\rho_\mathrm{M};\eta_\mathrm{t}\right) + l_0^{(\mathrm{F})d}\left(h_\mathrm{b}^2\rho + \frac{1}{N_\mathrm{f}}h^2\rho_\mathrm{M};\eta_\mathrm{b}\right)\right),
\end{aligned} \tag{5.42}$$

where primes denote derivatives with respect to the field invariant ρ. We extract the flow equations for the couplings in our truncation of the potential (Eq. (5.33)) with suitable differentiation and projection rules of the β function of the full potential, as seen for the simple toy model studied before. This flow equation agrees with the one found in [30] in the appropriate limit $h^2 \to 0$.
For the meson potential $v_k = k^{-d}V_k$ we get

$$\begin{aligned}
\partial_t v = &-dv + (d-2+\eta_\varphi)\,\rho_{\mathrm{M}} v' + (2d-4+2\eta_\varphi)\tau v_\tau + 2v_d\Big(N_{\mathrm{f}}^2 l_0^d\,(v';\eta_\varphi) \\
&+ \left(N_{\mathrm{f}}^2-1\right) l_0^d\left(m_\tau^2;\eta_\varphi\right) + l_0^d\,(v'+2\rho_{\mathrm{M}}v'';\eta_\varphi)\,\Big) \\
&- 2v_d d_\gamma N_{\mathrm{c}}\Bigg(l_0^{(\mathrm{F})d}\left(\frac{1}{N_{\mathrm{f}}}h^2(\rho_{\mathrm{M}}+\sqrt{\tau})+h_{\mathrm{t}}^2\rho;\eta_{\mathrm{t}}\right) + l_0^{(\mathrm{F})d}\left(\frac{1}{N_{\mathrm{f}}}h^2(\rho_{\mathrm{M}}+\sqrt{\tau})+h_{\mathrm{b}}^2\rho;\eta_{\mathrm{b}}\right) \\
&+ (N_{\mathrm{f}}-3) l_0^{(\mathrm{F})d}\left(\frac{1}{N_{\mathrm{f}}}h^2(\rho_{\mathrm{M}}+\sqrt{\tau});\eta_\psi\right) + l_0^{(\mathrm{F})d}\left(\frac{1}{N_{\mathrm{f}}}h^2(\rho_{\mathrm{M}}-(N_{\mathrm{f}}-1)\sqrt{\tau});\eta_\psi\right)\Bigg).
\end{aligned} \tag{5.43}$$

Here we have introduced $m_\tau^2 = v' + \frac{1}{N_{\mathrm{f}}}\rho_{\mathrm{M}} v_\tau$, and primes denote derivatives with respect to the field invariant ρ_{M}, while v_τ is the derivative with respect to τ. We project onto the different couplings in the potential, as done for the first model, through differentiation of this flow equation, yielding the flow equations of said couplings. This β function agrees with the one given in [33] in the limit $h_{\mathrm{t}}^2, h_{\mathrm{b}}^2 \to 0$.

The flow equation of the meson-fermion Yukawa coupling can be written as

$$
\begin{aligned}
\partial_t h^2 = \quad & (d-4+2\eta_\psi+\eta_\varphi)h^2 - \frac{4}{N_\mathrm{f}^2}h^4\Bigg[N_\mathrm{f}^2\Bigg(l_{1,1}^{(\mathrm{FB})d}\left(h_\mathrm{t}^2\kappa+\frac{1}{N_\mathrm{f}}h^2\kappa_\mathrm{M},v';\eta_\mathrm{t},\eta_\varphi\right)\\
& + l_{1,1}^{(\mathrm{FB})d}\left(h_\mathrm{b}^2\kappa+\frac{1}{N_\mathrm{f}}h^2\kappa_\mathrm{M},v';\eta_\mathrm{b},\eta_\varphi\right)+(N_\mathrm{f}-2)l_{1,1}^{(\mathrm{FB})d}\left(\frac{1}{N_\mathrm{f}}h^2\kappa_\mathrm{M},v';\eta_\psi,\eta_\varphi\right)\Bigg)\\
& -(N_\mathrm{f}^2-1)\Bigg(l_{1,1}^{(\mathrm{FB})d}\left(h_\mathrm{t}^2\kappa+\frac{1}{N_\mathrm{f}}h^2\kappa_\mathrm{M},m_\tau^2;\eta_\mathrm{t},\eta_\varphi\right)\\
& + l_{1,1}^{(\mathrm{FB})d}\left(h_\mathrm{b}^2\kappa+\frac{1}{N_\mathrm{f}}h^2\kappa_\mathrm{M},m_\tau^2;\eta_\mathrm{b},\eta_\varphi\right)+(N_\mathrm{f}-2)l_{1,1}^{(\mathrm{FB})d}\left(\frac{1}{N_\mathrm{f}}h^2\kappa_\mathrm{M},m_\tau^2;\eta_\psi,\eta_\varphi\right)\Bigg)\\
& -\Bigg(l_{1,1}^{(\mathrm{FB})d}\left(h_\mathrm{t}^2\kappa+\frac{1}{N_\mathrm{f}}h^2\kappa_\mathrm{M},v'+2\rho_\mathrm{M}v'';\eta_\mathrm{t},\eta_\varphi\right)\\
& + l_{1,1}^{(\mathrm{FB})d}\left(h_\mathrm{b}^2\kappa+\frac{1}{N_\mathrm{f}}h^2\kappa_\mathrm{M},v'+2\rho_\mathrm{M}v'';\eta_\mathrm{b},\eta_\varphi\right)\\
& + (N_\mathrm{f}-2)l_{1,1}^{(\mathrm{FB})d}\left(\frac{1}{N_\mathrm{f}}h^2\kappa_\mathrm{M},v'+2\rho_\mathrm{M}v'';\eta_\psi,\eta_\varphi\right)\Bigg)\Bigg]\\
& - 8(3+\xi)C_2(N_\mathrm{c})v_d g^2h^2\frac{1}{N_\mathrm{f}}\Bigg(l_{1,1}^{(\mathrm{FB})d}\left(h_\mathrm{t}^2\kappa+\frac{1}{N_\mathrm{f}}h^2\rho_\mathrm{M},0;\eta_\mathrm{t},\eta_\mathrm{F}\right)\\
& + l_{1,1}^{(\mathrm{FB})d}\left(h_\mathrm{b}^2\kappa+\frac{1}{N_\mathrm{f}}h^2\rho_\mathrm{M},0;\eta_\mathrm{b},\eta_\mathrm{F}\right)+(N_\mathrm{f}-2)l_{1,1}^{(\mathrm{FB})d}\left(\frac{1}{N_\mathrm{f}}h^2\rho_\mathrm{M},0;\eta_\psi,\eta_\mathrm{F}\right)\Bigg).
\end{aligned}
\tag{5.44}
$$

Here $C_2(N_\mathrm{c}) = (N_\mathrm{c}^2-1)/(2N_\mathrm{c})$ denotes a Casimir operator of the gauge group. The scalar contribution of this flow equation ($\propto h^4$) coincides with the one found in [33] in the limit of vanishing top- and bottom-Yukawa couplings. The contributions stemming from the gauge sector ($\propto g^2$) agree with those found in [34].

The top-Yukawa flow equation is given by

$$\begin{aligned}
\partial_t h_{\mathrm{t}}^2 = \quad & (d-4+\eta_\phi+2\eta_{\mathrm{t}})\, h_{\mathrm{t}}^2 - 4v_d h_{\mathrm{t}}^4 \Bigg[\left(6\kappa u'' + 4\kappa^2 u'''\right) \\
& l_{1,2}^{(\mathrm{FB})d}\left(h_{\mathrm{t}}^2\kappa + \frac{1}{N_{\mathrm{f}}}h^2\kappa_{\mathrm{M}}, u' + 2\kappa u''; \eta_{\mathrm{t}}, \eta_\phi\right) - 2\kappa u'' l_{1,2}^{(\mathrm{FB})d}\left(h_{\mathrm{t}}^2\kappa + \frac{1}{N_{\mathrm{f}}}h^2\kappa_{\mathrm{M}}, u'; \eta_{\mathrm{t}}, \eta_\phi\right) \\
& + 2h_{\mathrm{t}}^2\kappa\Bigg(l_{2,1}^{(\mathrm{FB})d}\left(h_{\mathrm{t}}^2\kappa + \frac{1}{N_{\mathrm{f}}}h^2\kappa_{\mathrm{M}}, u' + 2\kappa u''; \eta_{\mathrm{t}}, \eta_\phi\right) \\
& - l_{2,1}^{(\mathrm{FB})d}\left(h_{\mathrm{t}}^2\kappa + \frac{1}{N_{\mathrm{f}}}h^2\kappa_{\mathrm{M}}, u'; \eta_{\mathrm{t}}, \eta_\phi\right)\Bigg) - l_{1,1}^{(\mathrm{FB})d}\left(h_{\mathrm{t}}^2\kappa + \frac{1}{N_{\mathrm{f}}}h^2\kappa_{\mathrm{M}}, u' + 2\kappa u''; \eta_{\mathrm{t}}, \eta_\phi\right) \\
& + l_{1,1}^{(\mathrm{FB})d}\left(h_{\mathrm{t}}^2\kappa + \frac{1}{N_{\mathrm{f}}}h^2\kappa_{\mathrm{M}}, u'; \eta_{\mathrm{t}}, \eta_\phi\right) - 2\frac{h_{\mathrm{b}}^2}{h_{\mathrm{t}}^2}\Big[- 2\kappa u'' l_{1,2}^{(\mathrm{FB})d}\left(h_{\mathrm{b}}^2\kappa + \frac{1}{N_{\mathrm{f}}}h^2\kappa_{\mathrm{M}}, u'; \eta_{\mathrm{b}}, \eta_\phi\right) \\
& - 2h_{\mathrm{b}}^2\kappa l_{2,1}^{(\mathrm{FB})d}\left(h_{\mathrm{b}}^2\kappa + \frac{1}{N_{\mathrm{f}}}h^2\kappa_{\mathrm{M}}, u'; \eta_{\mathrm{b}}, \eta_\phi\right) + l_{1,1}^{(\mathrm{FB})d}\left(h_{\mathrm{b}}^2\kappa + \frac{1}{N_{\mathrm{f}}}h^2\kappa_{\mathrm{M}}, u'; \eta_{\mathrm{b}}, \eta_\phi\right)\Big]\Bigg] \\
& - 8(3+\xi)C_2(N_{\mathrm{c}})v_d g^2 h_{\mathrm{t}}^2 l_{1,1}^{(\mathrm{FB})d}\left(h_{\mathrm{t}}^2\kappa + \frac{1}{N_{\mathrm{f}}}h^2\kappa_{\mathrm{M}}, 0; \eta_{\mathrm{t}}, \eta_{\mathrm{F}}\right),
\end{aligned} \tag{5.45}$$

while the β function of the bottom-Yukawa coupling is

$$\begin{aligned}
\partial_t h_{\mathrm{b}}^2 = \quad & (d-4+\eta_\phi+2\eta_{\mathrm{b}})\, h_{\mathrm{t}}^2 - 4v_d h_{\mathrm{b}}^4 \Bigg[\left(6\kappa u'' + 4\kappa^2 u'''\right) \\
& l_{1,2}^{(\mathrm{FB})d}\left(h_{\mathrm{b}}^2\kappa + \frac{1}{N_{\mathrm{f}}}h^2\kappa_{\mathrm{M}}, u' + 2\kappa u''; \eta_{\mathrm{b}}, \eta_\phi\right) - 2\kappa u'' l_{1,2}^{(\mathrm{FB})d}\left(h_{\mathrm{b}}^2\kappa + \frac{1}{N_{\mathrm{f}}}h^2\kappa_{\mathrm{M}}, u'; \eta_{\mathrm{b}}, \eta_\phi\right) \\
& + 2h_{\mathrm{b}}^2\kappa\Bigg(l_{2,1}^{(\mathrm{FB})d}\left(h_{\mathrm{b}}^2\kappa + \frac{1}{N_{\mathrm{f}}}h^2\kappa_{\mathrm{M}}, u' + 2\kappa u''; \eta_{\mathrm{b}}, \eta_\phi\right) \\
& - l_{2,1}^{(\mathrm{FB})d}\left(h_{\mathrm{b}}^2\kappa + \frac{1}{N_{\mathrm{f}}}h^2\kappa_{\mathrm{M}}, u'; \eta_{\mathrm{b}}, \eta_\phi\right)\Bigg) - l_{1,1}^{(\mathrm{FB})d}\left(h_{\mathrm{b}}^2\kappa + \frac{1}{N_{\mathrm{f}}}h^2\kappa_{\mathrm{M}}, u' + 2\kappa u''; \eta_{\mathrm{b}}, \eta_\phi\right) \\
& + l_{1,1}^{(\mathrm{FB})d}\left(h_{\mathrm{b}}^2\kappa + \frac{1}{N_{\mathrm{f}}}h^2\kappa_{\mathrm{M}}, u'; \eta_{\mathrm{b}}, \eta_\phi\right) - 2\frac{h_{\mathrm{t}}^2}{h_{\mathrm{b}}^2}\Big[- 2\kappa u'' l_{1,2}^{(\mathrm{FB})d}\left(h_{\mathrm{t}}^2\kappa + \frac{1}{N_{\mathrm{f}}}h^2\kappa_{\mathrm{M}}, u'; \eta_{\mathrm{t}}, \eta_\phi\right) \\
& - 2h_{\mathrm{t}}^2\kappa l_{2,1}^{(\mathrm{FB})d}\left(h_{\mathrm{t}}^2\kappa + \frac{1}{N_{\mathrm{f}}}h^2\kappa_{\mathrm{M}}, u'; \eta_{\mathrm{t}}, \eta_\phi\right) + l_{1,1}^{(\mathrm{FB})d}\left(h_{\mathrm{t}}^2\kappa + \frac{1}{N_{\mathrm{f}}}h^2\kappa_{\mathrm{M}}, u'; \eta_{\mathrm{t}}, \eta_\phi\right)\Big]\Bigg] \\
& - 8(3+\xi)C_2(N_{\mathrm{c}})v_d g^2 h_{\mathrm{b}}^2 l_{1,1}^{(\mathrm{FB})d}\left(h_{\mathrm{b}}^2\kappa + \frac{1}{N_{\mathrm{f}}}h^2\kappa_{\mathrm{M}}, 0; \eta_{\mathrm{b}}, \eta_{\mathrm{F}}\right).
\end{aligned} \tag{5.46}$$

The scalar contributions to these equations agree with the ones found in [30], again in the limit of vanishing meson-Yukawa coupling h^2, while the gauge contributions

agree with the one given in [34].
The evolution of the wavefunction renormalizations Z_ϕ, Z_φ and Z_ψ^a will be followed by the respective anomalous dimensions $\eta_i = -\partial_t \log(Z_i)$. The one of the Higgs scalar is given by

$$\begin{aligned}\eta_\phi = \quad & \frac{8v_d}{d}\kappa\left[3u''m_{4,0}^d\left(u',0;\eta_\phi\right)+\left(3u''+2\kappa u'''\right)^2 m_{4,0}^d\left(u'+2\kappa u'',0;\eta_\phi\right)\right] \\ & -\frac{4d_\gamma}{d}v_d\Bigg[\kappa h_{\mathrm{t}}^4 m_2^{(\mathrm{F})d}\left(h_{\mathrm{t}}^2\kappa+\frac{1}{N_{\mathrm{f}}}h^2\kappa_{\mathrm{M}};\eta_{\mathrm{t}}\right)-h_{\mathrm{t}}^2 m_4^{(\mathrm{F})d}\left(h_{\mathrm{t}}^2\kappa+\frac{1}{N_{\mathrm{f}}}h^2\kappa_{\mathrm{M}};\eta_{\mathrm{t}}\right) \\ & +h_{\mathrm{b}}^4\kappa m_2^{(\mathrm{F})d}\left(h_{\mathrm{b}}^2\kappa+\frac{1}{N_{\mathrm{f}}}h^2\kappa_{\mathrm{M}};\eta_{\mathrm{b}}\right)-h_{\mathrm{b}}^2 m_4^{(\mathrm{F})d}\left(h_{\mathrm{b}}^2\kappa+\frac{1}{N_{\mathrm{f}}}h^2\kappa_{\mathrm{M}};\eta_{\mathrm{b}}\right)\Bigg],\end{aligned} \tag{5.47}$$

coinciding with the one give in [30] in the appropriate limit.
The scalar anomalous dimension of the Hubbard-Stratonovich field reads

$$\begin{aligned}\eta_\varphi = \quad & 8\frac{v_d}{d}\kappa_{\mathrm{M}}\left[2\lambda_1^2 m_{2,2}^d\left(v',v'+2\rho_{\mathrm{M}}v'';\eta_\varphi\right)+\frac{N_{\mathrm{f}}^2-2}{4}\lambda_2^2 m_{2,2}^d\left(v',m_\tau^2;\eta_\varphi\right)\right] \\ & +4d_\gamma\frac{v_d}{d}\frac{N_{\mathrm{c}}}{N_{\mathrm{f}}}h^2\Big(m_4^{(\mathrm{F})d}\left(h_{\mathrm{t}}^2\kappa+\frac{1}{N_{\mathrm{f}}}h^2\kappa_{\mathrm{M}};\eta_{\mathrm{t}}\right)+m_4^{(\mathrm{F})d}\left(h_{\mathrm{b}}^2\kappa+\frac{1}{N_{\mathrm{f}}}h^2\kappa_{\mathrm{M}};\eta_{\mathrm{b}}\right) \\ & +(N_{\mathrm{f}}-2)m_4^{(\mathrm{F})d}\left(\frac{1}{N_{\mathrm{f}}}h^2\kappa_{\mathrm{M}};\eta_\psi\right)\Big),\end{aligned} \tag{5.48}$$

agreeing with [33], again for vanishing h_{b}^2 and h_{t}^2.
The contribution to the fermion anomalous dimension coming from the meson sector

is

$$\begin{aligned}
\eta_{\psi,\mathrm{M}} = \quad & \frac{4}{N_\mathrm{f}^2}\frac{v_d}{d}h^2\Bigg[N_\mathrm{f}^2\Bigg(m_{1,2}^{(\mathrm{FB})d}\left(h_\mathrm{t}^2\kappa+\frac{1}{N_\mathrm{f}}h^2\kappa_\mathrm{M},v';\eta_\mathrm{t},\eta_\varphi\right)\\
&+m_{1,2}^{(\mathrm{FB})d}\left(h_\mathrm{b}^2\kappa+\frac{1}{N_\mathrm{f}}h^2\kappa_\mathrm{M},v';\eta_\mathrm{b},\eta_\varphi\right)+(N_\mathrm{f}-2)m_{1,2}^{(\mathrm{FB})d}\left(\frac{1}{N_\mathrm{f}}h^2\kappa_\mathrm{M},v';\eta_\psi,\eta_\varphi\right)\Bigg)\\
&+(N_\mathrm{f}^2-1)\Bigg(m_{1,2}^{(\mathrm{FB})d}\left(h_\mathrm{t}^2\kappa+\frac{1}{N_\mathrm{f}}h^2\kappa_\mathrm{M},m_\tau^2;\eta_\mathrm{t},\eta_\varphi\right)\\
&+m_{1,2}^{(\mathrm{FB})d}\left(h_\mathrm{b}^2\kappa+\frac{1}{N_\mathrm{f}}h^2\kappa_\mathrm{M},m_\tau^2;\eta_\mathrm{b},\eta_\varphi\right)\\
&+(N_\mathrm{f}-2)m_{1,2}^{(\mathrm{FB})d}\left(\frac{1}{N_\mathrm{f}}h^2\kappa_\mathrm{M},m_\tau^2;\eta_\psi,\eta_\varphi\right)\Bigg)\\
&+\Bigg(m_{1,2}^{(\mathrm{FB})d}\left(h_\mathrm{t}^2\kappa+\frac{1}{N_\mathrm{f}}h^2\kappa_\mathrm{M},v'+2\rho_\mathrm{M}v'';\eta_\mathrm{t},\eta_\varphi\right)\\
&+m_{1,2}^{(\mathrm{FB})d}\left(h_\mathrm{b}^2\kappa+\frac{1}{N_\mathrm{f}}h^2\kappa_\mathrm{M},v'+2\rho_\mathrm{M}v'';\eta_\mathrm{b},\eta_\varphi\right)\\
&+(N_\mathrm{f}-2)m_{1,2}^{(\mathrm{FB})d}\left(\frac{1}{N_\mathrm{f}}h^2\kappa_\mathrm{M},v'+2\rho_\mathrm{M}v'';\eta_\psi,\eta_\varphi\right)\Bigg)\Bigg],
\end{aligned} \tag{5.49}$$

which also agrees with the one found in [33]. The contributions of the gauge sector are given by

$$\begin{aligned}
\eta_{\psi,\mathrm{G}} = 8C_2(N_\mathrm{c})\frac{v_d}{d}g^2\Bigg[\quad & (3-\xi)m_{1,2}^{(\mathrm{FB})d}\left(\frac{1}{N_\mathrm{f}}h^2\kappa_\mathrm{M},0;\eta_\psi,\eta_\mathrm{F}\right)\\
&-3(1-\xi)\tilde{m}_{1,1}^{(\mathrm{FB})d}\left(\frac{1}{N_\mathrm{f}}h^2\kappa_\mathrm{M},0;\eta_\psi,\eta_\mathrm{F}\right)\Bigg],
\end{aligned} \tag{5.50}$$

coinciding with the one found in [34]. The scalar contribution of the Higgs doublet to the anomalous dimension of the left-handed doublet ψ_L can be summed up by

$$\begin{aligned}
\eta_\mathrm{L} = & \frac{4v_d}{d}\Bigg[h_\mathrm{t}^2\Big(m_{1,2}^{(\mathrm{FB})d}\left(h_\mathrm{t}^2\kappa+\frac{1}{N_\mathrm{f}}h^2\kappa_\mathrm{M},u';\eta_\mathrm{t},\eta_\phi\right)\\
&+m_{1,2}^{(\mathrm{FB})d}\left(h_\mathrm{t}^2\kappa+\frac{1}{N_\mathrm{f}}h^2\kappa_\mathrm{M},u'+2\kappa u'';\eta_\mathrm{t},\eta_\phi\right)\Big)\\
&+2h_\mathrm{b}^2m_{1,2}^{(\mathrm{FB})d}\left(h_\mathrm{b}^2\kappa+\frac{1}{N_\mathrm{f}}h^2\kappa_\mathrm{M},u';\eta_\mathrm{b},\eta_\phi\right)\Bigg],
\end{aligned} \tag{5.51}$$

while the ones for the right-handed components of top and bottom quark read

$$\begin{aligned}\eta_{\mathrm{R}}^{\mathrm{t}} =& \frac{4v_d}{d}h_{\mathrm{t}}^2\Big[m_{1,2}^{(\mathrm{FB})d}\left(h_{\mathrm{t}}^2\kappa+\frac{1}{N_{\mathrm{f}}}h^2\kappa_{\mathrm{M}},u';\eta_{\mathrm{t}},\eta_\phi\right)\\ &+m_{1,2}^{(\mathrm{FB})d}\left(h_{\mathrm{t}}^2\kappa+\frac{1}{N_{\mathrm{f}}}h^2\kappa_{\mathrm{M}},u'+2\kappa u'';\eta_{\mathrm{t}},\eta_\phi\right)\\ &+2m_{1,2}^{(\mathrm{FB})d}\left(h_{\mathrm{b}}^2\kappa+\frac{1}{N_{\mathrm{f}}}h^2\kappa_{\mathrm{M}},u';\eta_{\mathrm{b}},\eta_\phi\right)\Big],\end{aligned} \tag{5.52}$$

$$\begin{aligned}\eta_{\mathrm{R}}^{\mathrm{b}} =& \frac{4v_d}{d}h_{\mathrm{b}}^2\Big[m_{1,2}^{(\mathrm{FB})d}\left(h_{\mathrm{b}}^2\kappa+\frac{1}{N_{\mathrm{f}}}h^2\kappa_{\mathrm{M}},u';\eta_{\mathrm{b}},\eta_\phi\right)\\ &+m_{1,2}^{(\mathrm{FB})d}\left(h_{\mathrm{b}}^2\kappa+\frac{1}{N_{\mathrm{f}}}h^2\kappa_{\mathrm{M}},u'+2\kappa u'';\eta_{\mathrm{b}},\eta_\phi\right)\\ &+2m_{1,2}^{(\mathrm{FB})d}\left(h_{\mathrm{t}}^2\kappa+\frac{1}{N_{\mathrm{f}}}h^2\kappa_{\mathrm{M}},u';\eta_{\mathrm{t}},\eta_\phi\right)\Big].\end{aligned} \tag{5.53}$$

These equations agree with the ones found in [30], again in the limit of vanishing meson-Yukawa coupling h^2. The contributions from the meson and gauge sector to these two anomalous dimensions are given by

$$\begin{aligned}\eta_{\mathrm{GM}}^{\mathrm{t}} =& \quad \eta_\psi + 8C_2(N_{\mathrm{c}})\frac{v_d}{d}g^2\Bigg[(3-\xi)m_{1,2}^{(\mathrm{FB})d}\left(h_{\mathrm{t}}^2\kappa+\frac{1}{N_{\mathrm{f}}}h^2\kappa_{\mathrm{M}},0;\eta_{\mathrm{t}},\eta_{\mathrm{F}}\right)\\ &-3(1-\xi)\tilde{m}_{1,1}^{(\mathrm{FB})d}\left(h_{\mathrm{t}}^2\kappa+\frac{1}{N_{\mathrm{f}}}h^2\kappa_{\mathrm{M}},0;\eta_{\mathrm{t}},\eta_{\mathrm{F}}\right)\Bigg],\end{aligned} \tag{5.54}$$

$$\begin{aligned}\eta_{\mathrm{GM}}^{\mathrm{b}} =& \quad \eta_{\psi,\mathrm{M}} + 8C_2(N_{\mathrm{c}})\frac{v_d}{d}g^2\Bigg[(3-\xi)m_{1,2}^{(\mathrm{FB})d}\left(h_{\mathrm{b}}^2\kappa+\frac{1}{N_{\mathrm{f}}}h^2\kappa_{\mathrm{M}},0;\eta_{\mathrm{b}},\eta_{\mathrm{F}}\right)\\ &-3(1-\xi)\tilde{m}_{1,1}^{(\mathrm{FB})d}\left(h_{\mathrm{b}}^2\kappa+\frac{1}{N_{\mathrm{f}}}h^2\kappa_{\mathrm{M}},0;\eta_{\mathrm{b}},\eta_{\mathrm{F}}\right)\Bigg].\end{aligned} \tag{5.55}$$

We then define the anomalous dimension of the top, bottom and remaining quarks through

$$\eta_{\mathrm{t}} = \frac{1}{2}\left(\eta_{\mathrm{L}}+\eta_{\mathrm{R}}^{\mathrm{t}}\right)+\eta_{\mathrm{GM}}^{\mathrm{t}}, \tag{5.56}$$

$$\eta_{\mathrm{b}} = \frac{1}{2}\left(\eta_{\mathrm{L}}+\eta_{\mathrm{R}}^{\mathrm{b}}\right)+\eta_{\mathrm{GM}}^{\mathrm{b}}, \tag{5.57}$$

and

$$\eta_\psi = \eta_{\psi,\mathrm{M}}+\eta_{\psi,\mathrm{G}}. \tag{5.58}$$

All equations agree with the ones from the literature in the appropriate limits. For the chiral Higgs-top-bottom model we have to set g^2 and h^2 to zero and compare

the flow equations to the ones found in [30] while for the quark-meson model we have to set g, h_t and h_b to zero when checking against the equations obtained in [33]. The gauge sector can be checked in [34].
For the gauge sector we will use a (modified) perturbative two-loop equation for the running of the gauge coupling. Since this β function produces a Landau pole when integrating towards the infrared, we modify this flow such that we obtain an IR fixed point $\alpha_* = g_*^2/(4\pi)$ for that coupling [35]. This fixed point has to be chosen above the critical gauge coupling needed to induce chiral symmetry breaking, for our computations we choose it to be of order one, $\alpha_* = 2.5$ [34]. This is a somewhat crude approximation, but accurately modeling the IR behavior of the strong gauge sector has its own difficulties. The flow equation of the gauge coupling then reads

$$\partial_t g^2 = \eta_\mathrm{F} g^2 = -2\left(c_1 \frac{g^4}{16\pi^2} + c_2 \frac{g^6}{(16\pi^2)^2}\right)\left(1 - \exp\left(\frac{1}{\alpha_*} - \frac{1}{\frac{g^2}{4\pi}}\right)\right) \tag{5.59}$$

where we have introduced the constants

$$\begin{aligned} c_1 &= \left(\frac{11}{3}N_\mathrm{c} - \frac{2}{3}N_\mathrm{f}\right), \\ c_2 &= \left(\frac{34}{3}N_\mathrm{c}^2 - \frac{10}{3}N_\mathrm{c}N_\mathrm{f} - 2C_2(N_\mathrm{c})N_\mathrm{f}\right). \end{aligned} \tag{5.60}$$

Additional Contributions to the Flow Equations

Since the meson field φ^{ab} is not a fundamental field but originates from the Hubbard-Stratonovich transformation, this fermion-boson translation yields additional contributions to the flow equations of the meson sector, as shown in the previous section. With the functions parametrising the scale dependence of that Hubbard-Stratonivic field (Eqs. (5.23) and (5.24)) we get the additional contributions [34]

$$\partial_t \epsilon_\mathrm{M}|_\mathrm{add} = 2\frac{\epsilon_\mathrm{M}}{h^2}(1+\epsilon_\mathrm{M})(1+(1+\epsilon_\mathrm{M})Q_\sigma)(\beta_{\lambda_\sigma}^{g^4} g^4 + \beta_{\lambda_\sigma}^{g^2h^2}), \tag{5.61}$$

and for the Yukawa coupling

$$\partial_t h^2\Big|_\mathrm{add} = 2(1+2\epsilon_\mathrm{M} + Q_\sigma(1+\epsilon_\mathrm{M})^2)(\beta_{\lambda_\sigma}^{g^4} g^4 + \beta_{\lambda_\sigma}^{g^2h^2}) \tag{5.62}$$

in the symmetric phase. In the χSB regime, we similarly find

$$\partial_t \kappa_\mathrm{M}|_\mathrm{add} = 2\frac{\kappa_\mathrm{M}}{h^2}(1-\kappa_\mathrm{M}\lambda_1)(1+(1-\kappa_\mathrm{M}\lambda_1)Q_\sigma)(\beta_{\lambda_\sigma}^{g^4} g^4 + \beta_{\lambda_\sigma}^{g^2h^2}), \tag{5.63}$$

$$\partial_t h^2\Big|_\mathrm{add} = 2(1-2\kappa_\mathrm{M}\lambda_1 + Q_\sigma(1-\kappa_\mathrm{M}\lambda_1)^2)(\beta_{\lambda_\sigma}^{g^4} g^4 + \beta_{\lambda_\sigma}^{g^2h^2}). \tag{5.64}$$

The quantity $Q_\sigma = \partial_t(\bar{\lambda}_\sigma(k^2) - \bar{\lambda}_\sigma(0))/\partial_t\bar{\lambda}_\sigma(0)$ introduced here is a measure for the suppression of $\bar{\lambda}_\sigma(k^2)$ for large external momenta. Suppression implies $Q_\sigma < 0$, and in the χSB regime, where fermions are massive, non-pointlike four-fermion interactions will be suppressed by the inverse fermion mass squared [34]. We therefore choose

$$Q_\sigma = Q_\sigma^0 m_{1,2}^{(\mathrm{FB})d}\left(\frac{1}{N_\mathrm{f}}h^2\kappa_\mathrm{M}, 0; \eta_\psi, \eta_\mathrm{F}\right), \qquad Q_\sigma^0 < 0. \tag{5.65}$$

Tests for various different values of Q_σ^0 in the range $[-0.2, 0.001]$ show that results are qualitatively independent of the precise choice.

Removing the Massless Modes from the Spectrum

Since the symmetry broken by the Higgs mechanism is a global symmetry in the present model, there will be massless Goldstone bosons in our physical spectrum [36–38]. This is in contrast to the standard model where the Higgs mechanism breaks a gauge symmetry and the would-be Goldstone bosons mix with the weak vector bosons. This turns the gauge bosons massive and no Goldstone modes are left in the spectrum. To stay close to the standard model we have to remove these massless modes since these can significantly change the IR behavior of the model. This can be seen by looking at the threshold functions which encode the mass dependence and decoupling of massive modes from the RG flows. In the case of the linear regulator which we use in this work, this dependence is given by

$$\left(\frac{k^2}{k^2 + m^2}\right)^\alpha, \tag{5.66}$$

with some power α. While for large k the difference between massive and massless modes is negligible, we see that for $k \to 0$ they differ substantially: When looking at massive modes $m^2 \neq 0$ all threshold functions vanish and the modes decouple, leading to a freeze out of the flows in the IR. Contrary to this, massless modes do contribute to the flows on all scales k leading to the aforementioned differences in the IR behavior. These Goldstone modes can be directly identified by their mass argument $m^2/k^2 \sim u'(\kappa)$ in the threshold functions, since in the broken regime this vanishes at the minimum of the potential. Thus replacing the mass argument $u' \to u' + \omega v_k$ for some ω artificially makes these modes massive in the broken regime. v_k denotes the running of the vacuum expectation value, and ω is chosen such that the modes have a mass of the order of the W bosons, $\omega = (80/246)^2$.
The same problem occurs in the broken regime of the meson potential, where in the χSB phase we have N_f^2 massless modes which can be identified by their mass argument v'. These would-be massless states correspond to the meson spectrum in QCD. In the standard model, the masses of all these states are lifted by explicit breaking terms of the chiral symmetry, most prominently by the finite Yukawa

couplings to the Higgs sector. Whenever these would-be massless modes start influencing the flow, we, analogously to the scalars in the Higgs potential, insert one mass parameter γ for these Goldstone modes (like ω before) by hand, the influence of the precise choice on the IR observables of interest will be briefly discussed. For simplicity, we will choose only one mass for all these scalars and ignore the details of the flavor structure of the light quarks responsible for the different masses of the scalar and pseudoscalar mesons in the standard model.

5.4. Flows in the Full Model

For computations, we set $d = 4$, $d_\gamma = 4$, and we work in the Landau gauge $\xi = 0$, which is known to be a fixed point of the renormalization group [39]. Physical flows within the QCD domain are then determined by the initial conditions of the meson sector. Choosing

$$m_{\mathrm{M}}^2\Big|_{k=\Lambda} = \mathcal{O}(\Lambda^2), \qquad \lambda_{1,2}|_{k=\Lambda} = 0, \qquad \Big(Z_\varphi, h^2\Big)\Big|_{k=\Lambda} \to 0 \tag{5.67}$$

implies making the auxillary field super-heavy, non-dynamical and non-interacting at the UV scale Λ, thus decoupling from the rest of the theory and leaving us with only the standard QCD and Higgs sector flows. Having the fixed point strucure of Fig. 5.2 in mind, this corresponds to initial conditions far right of $\epsilon_{*,2}$, which are then attracted by this fixed point. Letting the system evolve towards the IR, the gauge coupling grows strong, and, when reaching the critical value of the gauge coupling g_{cr}^2, the meson sector becomes active, as depicted in Fig. 5.4.
The characteristic scale of strong interactions, Λ_{QCD}, is an energy scale solely determined through the renormalization group flow of g^2. In general this scale signals the breakdown of pertubation theory in QCD, indicated by a Landau pole in the perturbative β function of the strong gauge coupling. In this work, we define this scale through the asymptotic behavior of the flow of g^2

$$g^2(t) \sim \frac{g_0^2}{1 + c * t}, \qquad t = \log\Big(\frac{k}{\Lambda_0}\Big), \tag{5.68}$$

where Λ_0 is a high energy scale where the perturbative (one-loop) flow equation is valid. From this, we can determine Λ_{QCD} through

$$\Lambda_{\mathrm{QCD}} = \Lambda_0 \, \mathrm{e}^{-1/c}. \tag{5.69}$$

Chiral symmetry breaking induced by gauge interactions typically occurs at scales around Λ_{QCD}.
In our model, we can isolate flows of pure QCD by decoupling the Higgs scalar by making it very heavy, non-dynamical and setting the Higgs-top/bottom Yukawa couplings to zero.

$$m^2\Big|_{k=\Lambda} = \mathcal{O}(\Lambda^2), \qquad \Big(\lambda_\phi, h_{\mathrm{t}}^2, h_{\mathrm{b}}^2\Big)\Big|_{k=\Lambda} = 0, \qquad Z_\phi|_{k=\Lambda} \to 0. \tag{5.70}$$

We can then compare Λ_{QCD} to the masses generated through chiral symmetry breaking for different numbers of flavors N_{f}. These results are shown in Table 5.2. A first observation is that Λ_{QCD} is highly affected by the choice of N_{f}, as expected, since the running of the gauge coupling depends on the number of flavors. For

N_f	$m_{\chi\mathrm{SB}}$	Λ_QCD	$m_{\chi\mathrm{SB}}/\Lambda_\mathrm{QCD}$
1	31.5 GeV	33.4 GeV	94.3%
2	7.5 GeV	12.3 GeV	61.0%
3	1.7 GeV	3.9 GeV	43.6%
4	333 MeV	1.0 GeV	33.3%
5	48 MeV	212 MeV	22.6%
6	4.6 MeV	33 MeV	13.9%

Table 5.2.: Different masses generated through chiral symmetry breaking for varying number of flavors N_f. These masses were generated for a fixed value g_Λ which, for $N_\mathrm{f} = 6$, coincides with the initial condition necessary to achieve the physical value of g at the Z boson mass ($\alpha_\mathrm{s}(m_\mathrm{Z}) = 0.1185$). Analysis shows that the fraction $m_{\chi\mathrm{SB}}/\Lambda_\mathrm{QCD}$ is rather independent of the initial value of g, only affecting this ratio on the order of $\mathcal{O}(10\%)$, while of course Λ_QCD strongly depends on it. For smaller N_f the gauge coupling grows faster, implying larger Λ_QCD.

fewer flavors g grows large faster, thus the one-loop β function diverges at a larger scale. The fraction $m_{\chi\mathrm{SB}}/\Lambda_{\mathrm{QCD}}$ also decreases with increasing N_f which can be understood by looking at the flow equation of the meson potential (c.f. Eq. (5.43)), which symbolically reads

$$\partial_t v = \cdots + \#_1 N_\mathrm{f}^2 \text{ scalar contributions} - \#_2 N_\mathrm{f} \text{ fermionic contributions.} \quad (5.71)$$

The placeholders $\#_{1,2}$ are positive numbers, and contain the various couplings. We see that the scalar contributions enter with a positive sign, and scale with N_f^2, while the fermionic contributions only scale linearly in N_f and have a negative sign. It is these fermionic contributions which are, in addition to the gauge sector (see Eq. (5.61)), responsible for driving the system into the χSB phase. For larger N_f there are much more scalars in the theory (for $N_\mathrm{f} = 6$ our model contains 72 scalar fields), suppressing a fast development of a vev in the meson potential.

In the case where the scale at which the Higgs potential enters the broken regime is larger than Λ_{QCD}, the top and bottom quark acquire mass before the remaining quarks, and thus decouple from the flows. For this reason we set the number of flavors in the meson sector to from $N_\mathrm{f} = 6$ to $N_\mathrm{f} = 4$ at the SSB transition scale of the Higgs potential. We continue with the flow equations with reduced flavor number down towards the IR, continuously connecting the couplings at that transition. We will calculate the top/bottom mass through

$$m_{\mathrm{t/b}}^2 = \frac{1}{2} h_{\mathrm{t/b}}^2 \left(v^2 + v_\mathrm{M}^2 \right) + h^2 v_\mathrm{M}^2 \quad (5.72)$$

in that parameter region, where v denotes the vev of the Higgs potential and v_M the one of the meson potential. We have chosen the vev responsible for mass generation through the top/bottom Yukawa couplings to be a superposition of the Higgs and meson vacuum expectation values due to the overlapping nature of the respective field's quantum numbers. This is an ad hoc approximation to model the potentials. It is not naturally emerging from the flow equations since we have neglected the back reaction a condensate of one of the fields has on the other scalar field. A Higgs condensate for example implies mass terms for the top and bottom quark, given by $h_\mathrm{t} v(\bar{t}_\mathrm{L} t_\mathrm{R} + \bar{t}_\mathrm{R} t_\mathrm{L})$ and $h_\mathrm{b} v(\bar{t}_\mathrm{L} t_\mathrm{R} + \bar{t}_\mathrm{R} t_\mathrm{L})$, respectively. By means of the translation of quark bilinears to the meson field (c.f. Eq. (5.19)) this implies terms linear in some components of the matrix field, deforming the potential, and generate a vev at nonzero field also for the meson field. The same line of reasoning can be drawn in case of a chiral condensate, which then implies a nonzero Higgs vev. In case of large separation of these two scales (like in the standard model, $\Lambda_{\mathrm{QCD}} = \mathcal{O}(100\,\mathrm{MeV})$, $\Lambda_\mathrm{F} = \mathcal{O}(100 - 1000\,\mathrm{GeV})$), the top and bottom quark mass is dominated by the Higgs effect, since $v \gg v_\mathrm{M}$. If the scales are of similar magnitude however, the contribution to the masses stemming from chiral symmetry breaking

is not negligible anymore.
Should chiral symmetry breaking occur before the top and bottom quark gain masses through the Higgs effect, all quark masses are determined through χSB. Owing to the overlapping quantum numbers of some components of the meson field with the Higgs scalars, we model the Higgs vev to be the same as the meson vev in that case. The top/bottom mass are then given by

$$m_{\mathrm{t/b}}^2 = (\frac{1}{2}h_{\mathrm{t/b}}^2 + h^2)v_{\mathrm{M}}^2. \tag{5.73}$$

We do not need to adjust the number of flavors in this case, since all quarks gain masses and thus decouple at the same time.
Another adjustment done in the flows of the theory is that we dynamically change the number of active flavors in the running of the gauge coupling g^2. At the top mass threshold we reduce the number of active flavors in the β function from six to five. At the bottom mass, we again lower this by one, arriving at $N_{\mathrm{f}} = 4$ active flavors in the flow equation for scales lower than the bottom mass.
In Figures 5.3 and 5.4, example flows for initial conditions corresponding to parts of the standard model are depicted. By that we mean achieving a top mass of 173 GeV, a bottom mass of 4.2 GeV (not shown), a Fermi scale $v = 246\,\mathrm{GeV}$ and a strong gauge coupling at the Z boson mass of $\alpha(m_Z) = 0.1185$. Only the Higgs mass is different, since for that flow we initialized at $\lambda_{\phi,\Lambda} = 0$.

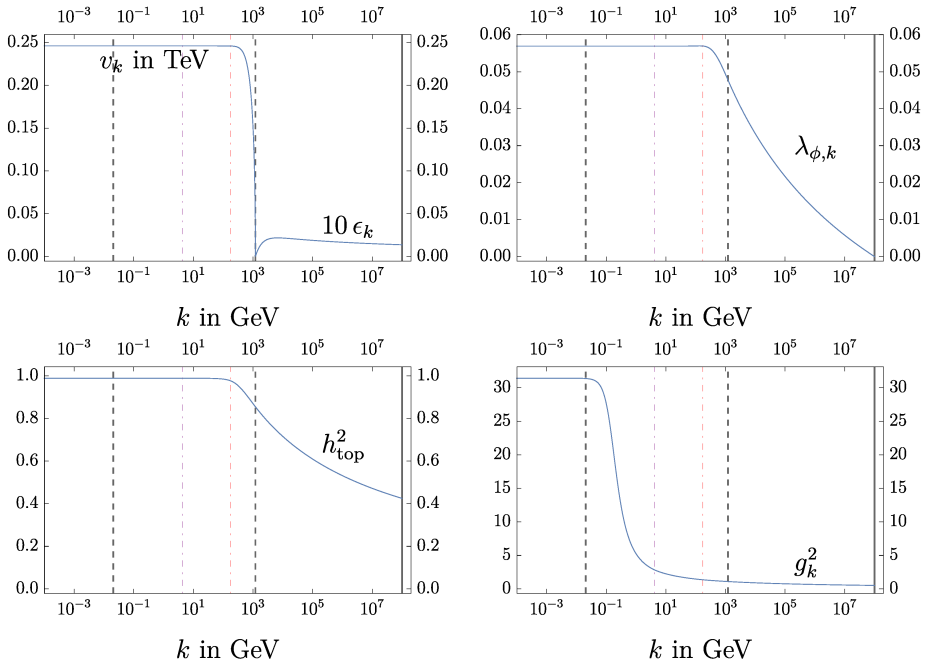

Figure 5.3.: Example flow of the couplings in the Higgs-top sector and the gauge sector of the toy model. The initial conditions for theses plots were chosen such that we have a vacuum expectation value of 246 GeV of the Higgs potential and the physical value of g^2 at the Z boson mass ($\alpha(m_Z) = 0.1185$). The dashed lines correspond to different threshold effects. At approximately 1 TeV (first grey dashed line) we enter the SSB regime of the Higgs potential. At that point we change the number of active flavors N_f in the meson sector from six to four. The red dotted line corresponds to the top mass, where we change the running of the gauge coupling to be driven by only 5 flavors. At the mass threshold of the bottom quark (purple dotted line), we again reduce the active flavors in the flow equation of the strong gauge coupling g^2 to four. We also see that the flows in the Higgs-top sector freeze out long before the meson field enters the broken regime (second dashed grey line) at around 20 MeV. The value of the IR fixed point in the β function of g^2 is choosen to be larger than the critical value necessary to trigger χSB (see Fig. 5.2), in our case we set it to $\alpha_* = 2.5$.

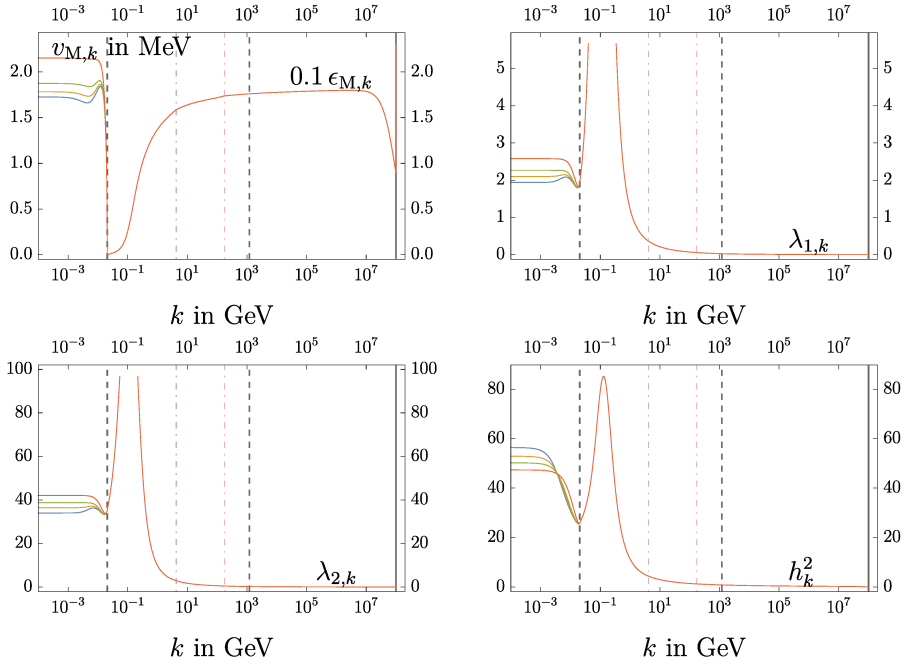

Figure 5.4.: Example flows of the couplings in the meson sector. The fixed-point structure of the meson couplings (c.f. Eq. (5.26)) can clearly be seen in the running of the dimensionless, renormalized mass parameter ϵ_M. The meson sector becomes active at around 1 GeV, indicated by a sudden increase of the Yukawa interaction h^2 and scalar self-interactions $\lambda_{1,2}$. The potential then quickly develops a non-vanishing minimum (second grey dashed line at around 20 MeV) and the flows freeze out. Here we depict flows for different values of the parameter γ removing the massless Goldstone modes from the spectrum ($\gamma = 0.5$: blue line, $\gamma = 1$: yellow line, $\gamma = 2$: green line, and $\gamma = 10$: red line). For the following computations we choose this parameter to be 1. This is chosen such that we get an IR value of the meson-Yukawa coupling to be around 7, comparable to the flows computed in [33]. The quark masses induced through chiral symmetry breaking $m_{\chi SB} = h_0 v_{M,0}$ are only slightly affected by this parameter, for the example flows given here they change on the order $\mathcal{O}(10\%)$.

5.5. Fine Tuning for Different Gauge Sectors

We now want to turn our attention to the influence of the gauge sector the so-called fine tuning problem. As already seen in the simple toy model studied in Section 4, we have to tune the initial condition of the relevant direction ϵ_Λ to a high accuracy in order to achieve a large scale separation between the UV initialization scale Λ and the Fermi scale v. In order to be able to compare theories with different gauge couplings, we keep all other marginal parameters fixed at initialization, chosen such that we get the correct values for the top and the bottom masses in the IR for the gauge coupling corresponding to the physical value, the scalar self interaction is set to zero, $\lambda_{\phi,\Lambda} = 0$. The initial conditions in the meson sector are chosen according to Eq. (5.67). We then vary the gauge coupling at the UV scale and look at the transition of the system from the phase dominated by χSB to the "deeply Higgsed" phase, where masses are generated mostly through the Higgs mechanism. Owing to the simplistic modelling of the scalar potentials in this first glimpse at the model, changing the number of flavors during the flow as well as, for the most part, ignoring the overlapping nature of the two fields, we are only confident to extract properties at that critical point for moderate values of the gauge couplings. We will mostly restrict ourselves to the parameter region where $\Lambda_{\mathrm{QCD}} \lesssim 0.1\Lambda_{\mathrm{F}}$, corresponding to a value of $g_{\Lambda,\mathrm{max}} \approx g_{\Lambda,\mathrm{Phys}} + 0.15$.
First we are interested in the influence of the different gauge couplings on the IR observable vacuum expectation value. For this we tune the relevant parameter ϵ to get a vev of 246 GeV, and then vary this around that special value ϵ_*. We find that stronger gauge interactions indeed lessen the fine tuning problem, indicated by a flattening of the slope for increasing g_Λ as shown in Figure 5.5.

The fine tuning problem is intimately related to the scaling exponent of the renormalization group, Θ. These critical exponents are the eigenvalues of the so-called stability matrix and characterize the behaviour of the associated coupling with respect to the energy scale. They are used to classify the different couplings in the theory. For more background and information regarding these RG exponents we refer the reader to the literature [15, 40, 41]. For the relevant parameter ϵ, this RG exponent is given by

$$\Theta = 2 - \eta, \tag{5.74}$$

with η being the anomalous dimension. This exponent can be related to the known critical exponents used to characterize phase transitions. Close to the critical point the behaviour of the order parameter $\langle\phi\rangle$ is given by

$$\langle\phi\rangle \sim |t|^\beta, \tag{5.75}$$

where β is the critical exponent of the order parameter and t is the control parameter of the system, $t = T - T_{\mathrm{C}}$ being the temperature in case of magnetic systems. In

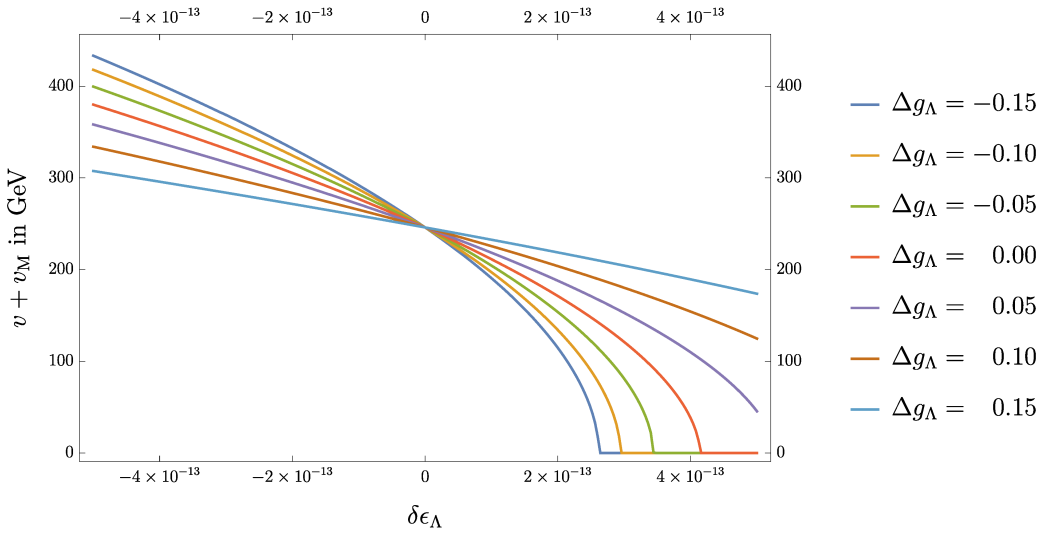

Figure 5.5.: Vacuum expectation value of the scalar fields, $v+v_M$, for different gauge couplings. The gauge couplings are plotted relative to the physical value of g, meaning we have $\alpha_S(m_Z) = 0.1185$. We normalized it to give the standard model value of 246 GeV at $\delta\epsilon_\Lambda = 0$, but of course the actual value of ϵ_Λ differs for each gauge coupling. We can see that for stronger interacting gauge sectors the slope becomes flatter, indicating a relaxing of the fine tuning necessary to achieve the desired separation of Λ and the vev.

our case, this control parameter is given by deviation of ϵ_Λ from its critical value, $t = \delta\epsilon_\Lambda$. Through hyperscaling relations known from thermodynamics [41], we can relate this critical exponent to two other critical exponents used to parametrize the power law behaviour of the correlation function, ν and η,

$$\beta = \frac{\nu}{2}\left(d - 2 + \eta\right). \tag{5.76}$$

The here introduced parameter ν is directly related to the RG exponent through

$$\nu = \frac{1}{\Theta} \tag{5.77}$$

and using Eq. (5.74) we obtain

$$\beta = \frac{1}{2}\left(1 + \eta + \mathcal{O}(\eta^2)\right), \tag{5.78}$$

where we have neglected higher order terms. The transition from one phase to the other is depicted in Figure 5.6. From these transitions we can obtain the critical

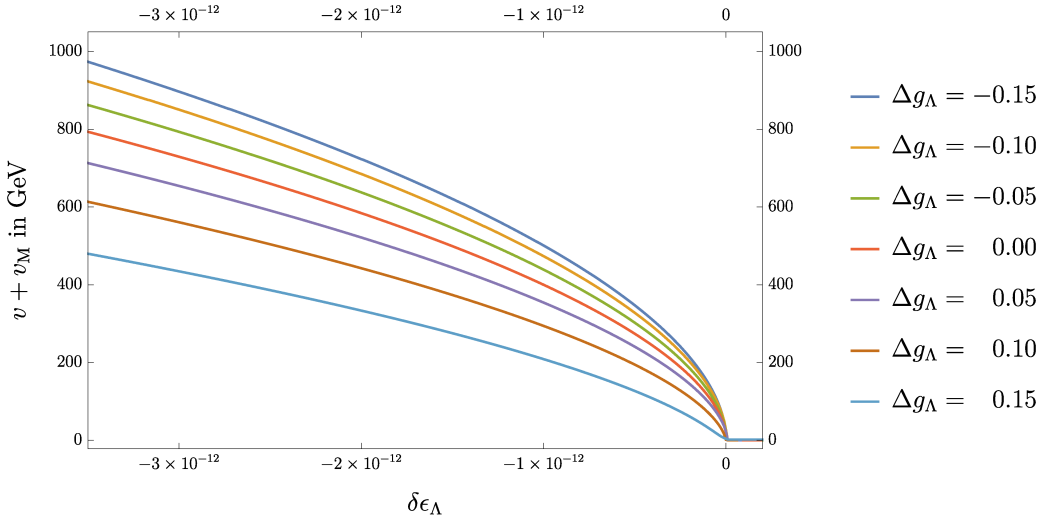

Figure 5.6.: Order Parameter $v + v_\mathrm{M}$ for different gauge couplings in the UV. As before, all other couplings were held fixed to the "physical" values and Δg denotes the deviation from the physical gauge coupling. We can see that the transition from the phase where masses are only generated through chiral symmetry breaking (positive $\delta\epsilon_\Lambda$) to the phase where we have a Higgs effect (negative $\delta\epsilon_\Lambda$) is sharper for smaller gauge couplings.

exponent, and thus the anomalous (scaling) dimension η (see Figure 5.7), which

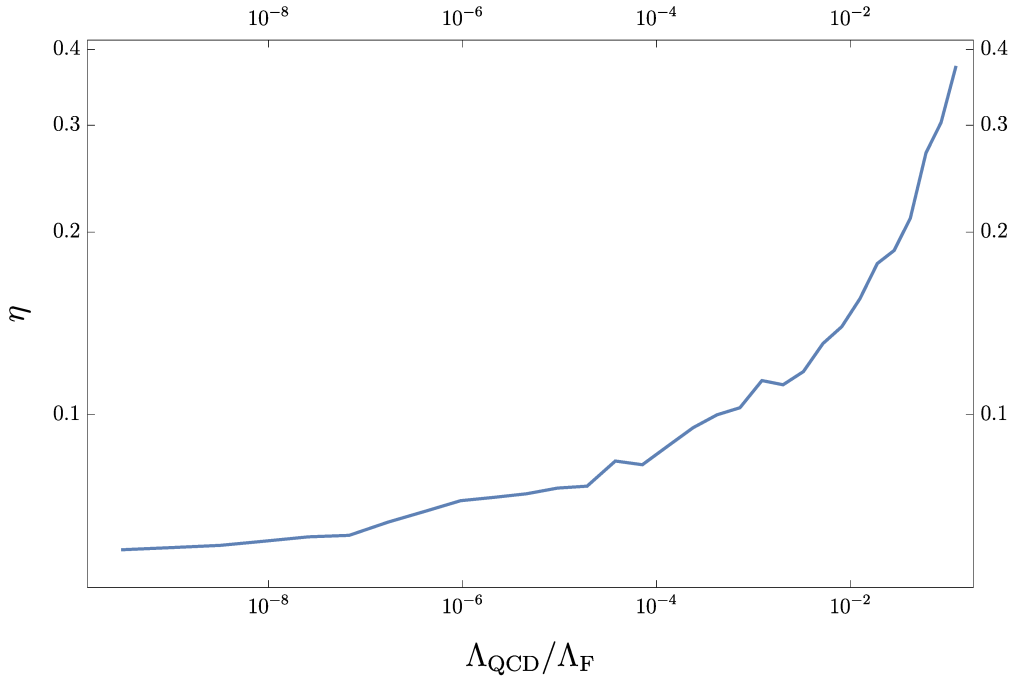

Figure 5.7.: The anomalous scaling dimension at the phase transition for different gauge couplings in the UV. The gauge couplings are translated to Λ_{QCD} via Eqs. (5.68) and (5.69), and we keep the Fermi scale $\Lambda_{\mathrm{F}} = 246$ GeV fixed. We see that for increasing ratio $\Lambda_{\mathrm{QCD}}/\Lambda_{\mathrm{F}}$ (increasing gauge coupling) the anomalous dimension grows, and the scaling exponent Θ decreases (c.f. Eq. (5.74)), relaxing the fine tuning problem. The noise in this curve is due to numerical errors, coming from the highly non-linear flow equations where an extreme precision for the initial values is necessary, together with the discrete logarithmic derivative used to extract the critical exponents in our study.

we do by numerically estimating the logarithmic derivative of v with respect to $\delta\epsilon_\Lambda$ in close proximity around the critical point. We observe good agreement with the expectations, since the anomalous dimension is proportional to $h^2_{\mathrm{t/b}}$. Keeping the Yukawa couplings fixed at the initialization scale Λ, an increase of the gauge coupling induces, through the contributions to the Yukawa coupling β functions (see Eqs. (5.45) and (5.46)), larger Yukawa couplings during the flow. This in turn increases the anomalous dimension, and slightly dampens the fine tuning problem.

Another feature of the strong interactions is te following: while in the "weak" coupling regime ($\Lambda_{\mathrm{QCD}} < \Lambda_{\mathrm{F}}$), the top mass changes only slightly for varying gauge sectors, the top and bottom mass are directly proportional to the scale of QCD in the case where we enter the strongly coupled phase quicker ($\Lambda_{\mathrm{QCD}} > \Lambda_{\mathrm{F}}$). This is, of course, originating from the fact that the vev of the meson potential, and thus the quark masses, are set by that scale. This is evident when looking at Figure 5.8, where at $\Lambda_{\mathrm{QCD}}/\Lambda_{\mathrm{F}} \approx 1$ the mass of the top quark starts to grow large, essentially being locked to be $\propto \Lambda_{\mathrm{QCD}}$. In this case we are able to study the case where $\Lambda_{\mathrm{QCD}} > \Lambda_{\mathrm{F}}$ since we are not interested in the phase transition at the quantum critical point, but instead look at observables in the deep IR. The way we model the scalar potentials has profound consequences on the SSB transition while the values of the couplings in the IR are not influenced by the different choices of parametrizing the overlapping quantum numbers of the two scalar fields.

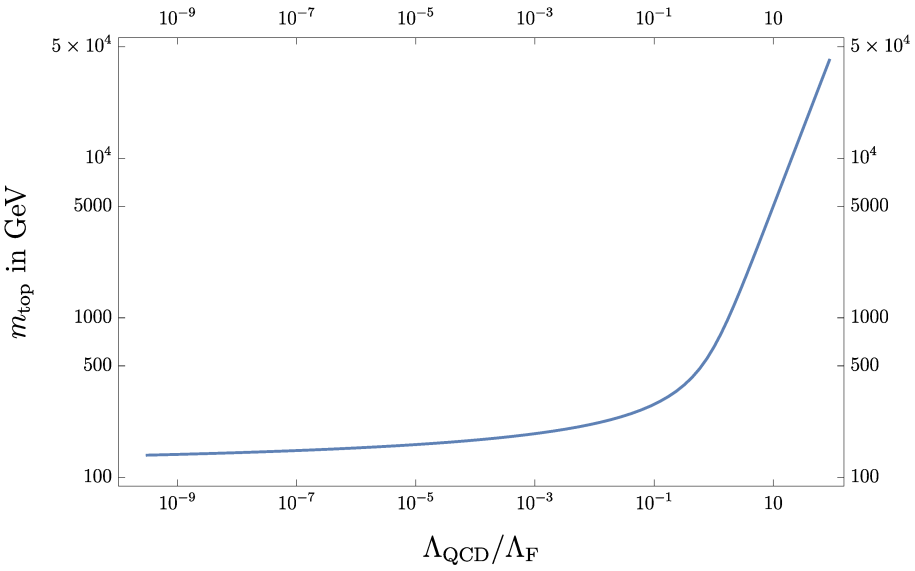

Figure 5.8.: Top mass for different ratios of $\Lambda_{\text{QCD}}/\Lambda_{\text{F}}$, with all other parameters fixed in the UV. We fine tune the control parameter such that we have a vacuum expectation value of $v = \sqrt{\Lambda_{\text{QCD}}^2 + \Lambda_{\text{F}}^2}$, with $\Lambda_{\text{F}} = 246$ GeV being fixed. This is chosen to model the overlapping nature of some of the fields quantum numbers. At $\Lambda_{\text{QCD}} \approx \Lambda_{\text{F}}$, the top mass gets mostly determined by Λ_{QCD} as is indicated by a linear behaviour in the plot.

6 Conclusion

In this work, we investigate two Yukawa toy models mimicking parts of the standard model. The prime focus is put on the so-called fine tuning problem inherently tied to scalar fields, present in the standard model by means of the Higgs boson. In Section 2 we briefly introduce the framework used in this work, the exact renormalization group, in particular the Wetterich equation. We introduce a very simple Yukawa theory containing one scalar field, as well as one Dirac fermion, and derive the flow equations using these non-perturbative methods in Section 3. In Section 4 we demonstrate the fine tuning problem as well as the issue of not being able to extend the theory to arbitrary high energies, at least in our truncation.
We then include the gauge sector, and in Section 5.1 and 5.2 present the tools necessary to deal with strongly interacting fermionic systems by means of the so-called Hubbard Stratonovich transformation. We arrive at the core model of interest for this work (Section 5.3), having a field content of one SU(2) doublet scalar field, playing the role of the Higgs field, two Dirac fermions coupled to that scalar, as well as four Dirac fermions not coupled to the Higgs scalar. The four-fermion interaction induced by QCD is encoded in an auxiliary scalar field. We extract the β functions of this model (Section 5.4) and investigate the effect of different scale separations between the Fermi scale and the characteristic scale of QCD, Λ_{QCD} on the fine tuning problem in Section 5.5.
We find that a stronger interacting gauge sector indeed lessens the fine-tuning problem, as is indicated by a reduction of the RG scaling exponent, classically given by $\Theta = 2$. Owing to the simplistic nature of our modelling of the scalar potentials, we restrict our analysis to cases where Λ_{QCD} is smaller than the Fermi scale set by the Higgs mechanism. For further analysis of even more strongly interacting gauge sectors, we will have to model the scalar potentials in a more precise way.
Investigating the fine-tuning problem in a new class of UV complete RG trajectories free of the triviality problem, recently constructed in [42, 43], is of interest and can be done in future works. For a more thorough study of the fine-tuning problem in

the standard model, the next step would be the inclusion of further contributions to the flow equations stemming from the electroweak gauge sector in the standard model, as could be done by perturbatively including them in the β functions of the present model. Another point to consider is the scheme dependence of the exact flow equations obtained through the Wetterich equation. An analysis for different regulator shape functions to give error estimates of the results would be of interest.

A Threshold Functions

Here we provide the expressions for all threshold functions used in the main text. These can be cross checked in [30, 33, 34, 44].

A.1. Definitions

We define the regularized kinetic terms in momentum space for bosons and fermions as

$$\begin{aligned} P(q) &= q^2 \left(1 + r_{k,\mathrm{B}}(q)\right), \\ P_{\mathrm{F}}(q) &= q^2 \left(1 + r_{k,\mathrm{F}}(q)\right)^2 = q^2 \left(1 + r_{k,\mathrm{L}}(q)\right)\left(1 + r_{k,\mathrm{R}}(q)\right), \end{aligned}$$

where for chiral fermions we have introduced regulator shape functions for the left- and right-handed part, respectively. The loop momentum integrations appearing on the right hand side of the Wetterich equations can then be encoded in threshold functions parametrizing the regulator dependece of the flow equations. The

threshold integral are given by

$$
\begin{aligned}
l_n^d\left(\omega;\eta_\phi\right) =& \frac{n+\delta_{n,0}}{4} v_d^{-1} k^{2n-d} \int_q \\
& \left[\left(\frac{1}{Z_\phi}\frac{\partial R_k(q)}{\partial t}\right)\frac{1}{\left(P(q)+\omega k^2\right)^{n+1}}\right], \\
l_n^{(\mathrm{F})d}\left(\omega;\eta_\psi\right) =& \frac{n+\delta_{n,0}}{2} v_d^{-1} k^{2n-d} \int_q \\
& \left[\frac{P_\mathrm{F}(q)}{1+r_{k,\mathrm{F}}(q)}\left(\frac{1}{Z_\psi}\frac{\partial(Z_\psi r_{k,\mathrm{F}}(q))}{\partial t}\right)\left(P_\mathrm{F}(q)+\omega k^2\right)^{-(n+1)}\right], \\
l_{n_1,n_2}^{(\mathrm{FB})d}\left(\omega_1,\omega_2;\eta_\psi,\eta_\phi\right) =& -\frac{1}{4} v_d^{-1} k^{2(n_1+n_2)-d} \int_q \\
& \tilde{\partial}_t\left[\frac{1}{\left(P_\mathrm{F}(q)+\omega_1 k^2\right)^{n_1}\left(P(q)+\omega_2 k^2\right)^{n_2}}\right], \\
l_{n_1,n_2,n_3}^{(\mathrm{FBB})d}\left(\omega_1,\omega_2,\omega_3;\eta_\psi,\eta_{\phi_1},\eta_{\phi_2}\right) =& -\frac{1}{4} v_d^{-1} k^{2(n_1+n_2+n_3)-d} \int_q \\
& \tilde{\partial}_t\left[\frac{1}{\left(P_\mathrm{F}(q)+\omega_1 k^2\right)^{n_1}\left(P(q)+\omega_2 k^2\right)^{n_2}\left(P(q)+\omega_3 k^2\right)^{n_3}}\right], \\
m_{n_1,n_2}^{d}\left(\omega_1,\omega_2;\eta_\phi\right) =& -\frac{1}{4} v_d^{-1} k^{2(n_1+n_2-1)-d} \int_q q^2 \\
& \tilde{\partial}_t\left[\frac{\left(\frac{\partial}{\partial q^2}P(q)\right)}{\left[P(q)+\omega_1 k^2\right]^{n_1}}\frac{\left(\frac{\partial}{\partial q^2}P(q)\right)}{\left[P(q)+\omega_2 k^2\right]^{n_2}}\right], \\
m_2^{(\mathrm{F})d}\left(\omega;\eta_\psi\right) =& -\frac{1}{4} v_d^{-1} k^{6-d} \int_q q^2 \tilde{\partial}_t\left[\frac{\left(\frac{\partial}{\partial q^2}P_\mathrm{F}(q)\right)}{\left[P_\mathrm{F}(q)+\omega k^2\right]^2}\right]^2, \\
m_4^{(\mathrm{F})d}\left(\omega;\eta_\psi\right) =& -\frac{1}{4} v_d^{-1} k^{4-d} \int_q q^4 \tilde{\partial}_t\left[\frac{\partial}{\partial q^2}\frac{1+r_{k,\mathrm{F}(q)}}{P_\mathrm{F}(q)+\omega k^2}\right]^2, \\
m_{n_1,n_2}^{(\mathrm{FB})d}\left(\omega_1,\omega_2;\eta_\psi,\eta_\phi\right) =& -\frac{1}{4} v_d^{-1} k^{2(n_1+n_2-1)-d} \int_q q^2 \\
& \tilde{\partial}_t\left[\frac{1+r_{k,\mathrm{F}}(q)}{\left[P_\mathrm{F}(q)+\omega_1 k^2\right]^{n_1}}\frac{\left(\frac{\partial}{\partial q^2}P(q)\right)}{\left[P(q)+\omega_2 k^2\right]^{n_2}}\right], \\
\tilde{m}_{1,1}^{(\mathrm{FB})d}\left(\omega_1,\omega_2;\eta_\psi,\eta_\phi\right) =& -\frac{1}{4} v_d^{-1} k^{4-d} \int_q \\
& \tilde{\partial}_t\left[\frac{1+r_{k,\mathrm{F}}(q)}{\left[P_\mathrm{F}(q)+\omega_1 k^2\right]^{1}}\frac{1}{\left[P(q)+\omega_2 k^2\right]^{1}}\right].
\end{aligned}
$$

The operator $\tilde{\partial}_t$ denotes differentiation with respect to RG time t, but only acts on the regulators. It can be defined through

$$\tilde{\partial}_t = \sum_i \int_x \frac{\partial_t \left(Z_i r_i(x) \right)}{Z_i} \frac{\delta}{\delta r_i(x)},$$

where we sum over all degrees of freedom i present in our truncation.

A.2. Linear Regulator Shape Function

Choosing the bosonic regulator shape functions to be the piecewise linear regulator [45]

$$r_{\mathrm{B}} \left(\frac{k^2}{q^2} - 1 \right) \Theta \left(k^2 - q^2 \right),$$

and defining the fermionic one to be

$$(1 + r_{\mathrm{B}}) = (1 + r_{\mathrm{L}})(1 + r_{\mathrm{R}}).$$

the threshold functions can be computed analytically, an enormous advantage for our numerical methods solving the flow equations, and read

$$
\begin{aligned}
l_n^d\left(\omega;\eta_\phi\right) =& \frac{2(\delta_{n,0}+n)}{d}\frac{1-\frac{\eta_\phi}{d+2}}{\left(1+\omega\right)^{n+1}},\\
l_n^{(\mathrm{F})d}\left(\omega;\eta_\psi\right) =& \frac{2(\delta_{n,0}+n)}{d}\frac{1-\frac{\eta_\psi}{d+1}}{\left(1+\omega\right)^{n+1}},\\
l_{n_1,n_2}^{(\mathrm{FB})d}\left(\omega_1,\omega_2;\eta_\psi,\eta_\phi\right) =& \frac{2}{d}\frac{1}{\left(1+\omega_1\right)^{n_1}\left(1+\omega_2\right)^{n_2}}\\
&\left[\frac{n_1}{1+\omega_1}\left(1-\frac{\eta_\psi}{d+1}\right)+\frac{n_2}{1+\omega_2}\left(1-\frac{\eta_\phi}{d+2}\right)\right],\\
l_{n_1,n_2,n_3}^{(\mathrm{FBB})d}\left(\omega_1,\omega_2,\omega_3;\eta_\psi,\eta_{\phi_1},\eta_{\phi_2}\right) =& \frac{2}{d}\frac{1}{\left(1+\omega_1\right)^{n_1}\left(1+\omega_2\right)^{n_2}\left(1+\omega_3\right)^{n_3}}\\
&\left[\frac{n_1}{1+\omega_1}\left(1-\frac{\eta_\psi}{d+1}\right)+\frac{n_2}{1+\omega_2}\left(1-\frac{\eta_{\phi_1}}{d+2}\right)\right.\\
&\left.+\frac{n_3}{1+\omega_3}\left(1-\eta_{\phi_2}\right)\right],\\
m_{n_1,n_2}^d\left(\omega_1,\omega_2;\eta_\phi\right) =& \frac{1}{\left(1+\omega_1\right)^{n_1}\left(1+\omega_2\right)^{n_2}},\\
m_2^{(\mathrm{F})d}\left(\omega;\eta_\psi\right) =& \frac{1}{\left(1+\omega\right)^4},\\
m_4^{(\mathrm{F})d}\left(\omega;\eta_\psi\right) =& \frac{1}{\left(1+\omega\right)^4}+\frac{1-\eta_\psi}{d-2}\frac{1}{\left(1+\omega\right)^3}\\
&-\left(\frac{1-\eta_\psi}{2d-4}+\frac{1}{4}\right)\frac{1}{\left(1+\omega\right)^2},\\
m_{n_1,n_2}^{(\mathrm{FB})d}\left(\omega_1,\omega_2;\eta_\psi,\eta_\phi\right) =& \left(1-\frac{\eta_\phi}{d+1}\right)\frac{1}{\left(1+\omega_1\right)^{n_1}\left(1+\omega_2\right)^{n_2}},\\
\tilde{m}_{1,1}^{(\mathrm{FB})d}\left(\omega_1,\omega_2;\eta_\psi,\eta_\phi\right) =& \frac{2}{d-1}\frac{1}{\left(1+\omega_1\right)\left(1+\omega_2\right)}\\
&\left(\frac{1-\frac{\eta_\phi}{d+1}}{1+\omega_2}+\frac{1-\frac{\eta_\psi}{d}}{1+\omega_1}-\frac{1}{2}+\frac{\eta_\psi}{2d}\right).
\end{aligned}
$$

Bibliography

[1] G. Aad et al. Observation of a new particle in the search for the Standard Model Higgs boson with the ATLAS detector at the LHC. *Physics Letters B*, 716(1):1–29, Sep 2012. ISSN 0370-2693. URL `http://dx.doi.org/10.1016/j.physletb.2012.08.020`.

[2] S. Chatrchyan et al. Observation of a new boson at a mass of 125 GeV with the CMS experiment at the LHC. *Physics Letters B*, 716(1):30–61, Sep 2012. ISSN 0370-2693. URL `http://dx.doi.org/10.1016/j.physletb.2012.08.021`.

[3] F. Englert and R. Brout. Broken Symmetry and the Mass of Gauge Vector Mesons. *Phys. Rev. Lett.*, 13:321–323, 1964.

[4] Peter W. Higgs. Broken symmetries, massless particles and gauge fields. *Phys. Lett.*, 12:132–133, 1964.

[5] Peter W. Higgs. Broken Symmetries and the Masses of Gauge Bosons. *Phys. Rev. Lett.*, 13:508–509, 1964.

[6] Peter W. Higgs. Spontaneous Symmetry Breakdown without Massless Bosons. *Phys. Rev.*, 145:1156–1163, 1966.

[7] Steven Weinberg. A Model of Leptons. *Phys. Rev. Lett.*, 19:1264–1266, 1967.

[8] Abdus Salam. Weak and Electromagnetic Interactions. *Conf. Proc. C*, 680519: 367–377, 1968.

[9] O. W. Greenberg. Spin and Unitary-Spin Independence in a Paraquark Model of Baryons and Mesons. *Phys. Rev. Lett.*, 13:598–602, Nov 1964. URL `https://link.aps.org/doi/10.1103/PhysRevLett.13.598`.

[10] M. Y. Han and Y. Nambu. Three-Triplet Model with Double SU(3) Symmetry. *Phys. Rev.*, 139:B1006–B1010, Aug 1965. URL `https://link.aps.org/doi/10.1103/PhysRev.139.B1006`.

[11] M. Gell-Mann. Quarks. *Acta Phys. Austriaca Suppl.*, 9:733–761, 1972.

[12] H. Fritzsch, Murray Gell-Mann, and H. Leutwyler. Advantages of the Color Octet Gluon Picture. *Phys. Lett. B*, 47:365–368, 1973.

[13] Steven Weinberg. *The Quantum Theory of Fields*, volume 1. Cambridge University Press, 1995.

[14] Steven Weinberg. *The Quantum Theory of Fields*, volume 2. Cambridge University Press, 1996.

[15] Jean Zinn-Justin. *Quantum Field Theory and Critical Phenomena; 4th ed.* Internat. Ser. Mono. Phys. Clarendon Press, Oxford, 2002. URL `https://cds.cern.ch/record/572813`.

[16] K.G. Wilson and John B. Kogut. The Renormalization group and the epsilon expansion. *Phys. Rept.*, 12:75–199, 1974.

[17] Holger Gies. Introduction to the functional RG and applications to gauge theories. *Lect. Notes Phys.*, 852:287–348, 2012.

[18] Christof Wetterich. Exact evolution equation for the effective potential. *Phys. Lett. B*, 301:90–94, 1993.

[19] Tim R. Morris. The Exact Renormalization Group and Approximate Solutions. *International Journal of Modern Physics A*, 09(14):2411–2449, Jun 1994. ISSN 1793-656X. URL `http://dx.doi.org/10.1142/S0217751X94000972`.

[20] M. Bonini, M. D'Attanasio, and G. Marchesini. Perturbative renormalization and infrared finiteness in the Wilson renormalization group: the massless scalar case. *Nuclear Physics B*, 409(2):441–464, Nov 1993. ISSN 0550-3213. URL `http://dx.doi.org/10.1016/0550-3213(93)90588-G`.

[21] Ulrich Ellwanger. Flow equations for n point functions and bound states. *Zeitschrift für Physik C Particles and Fields*, 62(3):503–510, Sep 1994. ISSN 1434-6052. URL `http://dx.doi.org/10.1007/BF01555911`.

[22] Clemens Gneiting. Higgs mass bounds from renormalization flow, 2005. URL `https://www.tpi.uni-jena.de/~gies/assets/theses/ClemensGneiting-Diplomarbeit.pdf`.

[23] René Sondenheimer. *Renormalization group flow of the Higgs sector*. PhD thesis, Friedrich-Schiller-Universität Jena, 2016. URL `https://www.db-thueringen.de/receive/dbt_mods_00029326`.

[24] Holger Gies, Clemens Gneiting, and René Sondenheimer. Higgs Mass Bounds from Renormalization Flow for a simple Yukawa model. *Phys. Rev. D*, 89(4): 045012, 2014.

[25] David J. Gross and Frank Wilczek. Ultraviolet Behavior of Non-Abelian Gauge Theories. *Phys. Rev. Lett.*, 30:1343–1346, Jun 1973. URL `https://link.aps.org/doi/10.1103/PhysRevLett.30.1343`.

[26] H. David Politzer. Reliable Perturbative Results for Strong Interactions? *Phys. Rev. Lett.*, 30:1346–1349, Jun 1973. URL `https://link.aps.org/doi/10.1103/PhysRevLett.30.1346`.

[27] Holger Gies, Joerg Jaeckel, and Christof Wetterich. Towards a renormalizable standard model without fundamental Higgs scalar. *Phys. Rev. D*, 69:105008, 2004.

[28] Jan M. Pawlowski. Aspects of the Functional Renormalization Group. *Annals Phys.*, 322:2831, 2007.

[29] Holger Gies and Christof Wetterich. Renormalization flow of bound states. *Physical Review D*, 65(6), Feb 2002. ISSN 1089-4918. URL `http://dx.doi.org/10.1103/PhysRevD.65.065001`.

[30] Holger Gies and René Sondenheimer. Higgs Mass Bounds from Renormalization Flow for a Higgs-top-bottom model. *Eur. Phys. J. C*, 75(2):68, 2015.

[31] Holger Gies, Stefan Rechenberger, Michael M. Scherer, and Luca Zambelli. An asymptotic safety scenario for gauged chiral Higgs–Yukawa models. *The European Physical Journal C*, 73(12), Nov 2013. ISSN 1434-6052. URL `http://dx.doi.org/10.1140/epjc/s10052-013-2652-y`.

[32] Lukas Janssen and Holger Gies. Critical behavior of the (2+1)-dimensional Thirring model. *Phys. Rev. D*, 86:105007, 2012.

[33] D.U. Jungnickel and C. Wetterich. Effective action for the chiral quark-meson model. *Phys. Rev. D*, 53:5142–5175, 1996.

[34] Holger Gies and Christof Wetterich. Universality of spontaneous chiral symmetry breaking in gauge theories. *Physical Review D*, 69(2), Jan 2004. ISSN 1550-2368. URL `http://dx.doi.org/10.1103/PhysRevD.69.025001`.

[35] Holger Gies. Running coupling in Yang-Mills theory: A flow equation study. *Phys. Rev. D*, 66:025006, 2002.

[36] J. Goldstone. Field Theories with Superconductor Solutions. *Nuovo Cim.*, 19: 154–164, 1961.

[37] Jeffrey Goldstone, Abdus Salam, and Steven Weinberg. Broken Symmetries. *Phys. Rev.*, 127:965–970, 1962.

[38] Sidney A. Bludman and Abraham Klein. Broken Symmetries and Massless Particles. *Phys. Rev.*, 131:2364–2372, 1963.

[39] Ulrich Ellwanger, Manfred Hirsch, and Axel Weber. Flow equations for the relevant part of the pure Yang-Mills action. *Z. Phys. C*, 69:687–698, 1996.

[40] Michael E. Peskin and Daniel V. Schroeder. *An Introduction to quantum field theory*. Addison-Wesley, Reading, USA, 1995. ISBN 978-0-201-50397-5.

[41] H. Kleinert and V. Schulte-Frohlinde. *Critical Properties of ϕ^4-theories*. World Scientific, 2001. ISBN 9789810246594. LCCN 20280526. URL `https://books.google.de/books?id=rBfWk4vVi-cC`.

[42] Holger Gies, René Sondenheimer, Alessandro Ugolotti, and Luca Zambelli. Asymptotic freedom in $\mathbb{Z}_2$-Yukawa-QCD models. *The European Physical Journal C*, 79(2), Jan 2019. ISSN 1434-6052. URL `http://dx.doi.org/10.1140/epjc/s10052-019-6604-z`.

[43] Holger Gies, René Sondenheimer, Alessandro Ugolotti, and Luca Zambelli. Scheme Dependence of Asymptotically Free Solutions. *The European Physical Journal C*, 79(6), Jun 2019. ISSN 1434-6052. URL `http://dx.doi.org/10.1140/epjc/s10052-019-6956-4`.

[44] Jürgen Berges, Nikolaos Tetradis, and Christof Wetterich. Non-perturbative renormalization flow in quantum field theory and statistical physics. *Physics Reports*, 363(4-6):223–386, Jun 2002. ISSN 0370-1573. URL `http://dx.doi.org/10.1016/S0370-1573(01)00098-9`.

[45] Daniel F. Litim. Optimized renormalization group flows. *Physical Review D*, 64(10), Oct 2001. ISSN 1089-4918. URL `http://dx.doi.org/10.1103/PhysRevD.64.105007`.

Danksagung

Zuerst möchte ich mich bei Professor Holger Gies bedanken. Sie haben mir die Möglichkeit gegeben, die Masterarbeit in diesem sehr interessanten Gebiet zu schreiben und hatten stets Zeit für Fragen und Probleme meinerseits.
Auch bei meinem Betreuer und Zweitkorrektor Dr. Luca Zambelli möchte ich mich bedanken, der trotz der nicht leichten Situation in diesem Jahr immer Zeit für Diskussionen und Anmerkungen hatte.
Auch danke ich meinen Freunden Simon Schreyer, Ruben Küspert, Felix Stehr und Franz Roeder für die Abo-Falle und Unterstützung im Studium. Insbesondere bedanke ich mich bei Simon Schreyer und Ruben Küspert für das Korrekturlesen und die hilfreichen Diskussionen.
Besonderer Dank gilt auch meinen Eltern für die Unterstützung im Studium.

Selbstständigkeit und Veröffentlichung

Ich erkläre, die vorliegende Arbeit selbstständig verfasst, und keine anderen als die angegebenen Quellen und Hilfsmittel verwendet zu haben.

Vonseiten des Verfassers bestehen keinerlei Einwände, diese Arbeit der Thüringer Universitäts- und Landesbibliothek zur öffentlichen Nutzung zur Verfügung zu stellen.

Jena, den 20. November 2020

Richard Schmieden